



A Typology of Antenna Tuner Control Schemes, for One or More Antennas

FRÉDÉRIC BROYDÉ¹, and
EVELYNE CLAVELIER²

¹Excem, 12 chemin des Hauts de Clairefontaine, 78580 Maule, France

²Eurexcem, 12 chemin des Hauts de Clairefontaine, 78580 Maule, France

Corresponding author: Frédéric Broydé (e-mail: fredbroyde@eurexcem.com).

ABSTRACT We identify five types of antenna tuner control scheme, which are suitable for a wireless transmitter using a single antenna. Four of them use a sensing unit measuring electrical variables either at the radio port or at the antenna port of the antenna tuner. We also define and discuss four types of antenna tuner control scheme which are relevant to a transmitter utilizing several antennas for MIMO radio transmission. The accuracy and other characteristics of the different schemes are discussed and compared.

INDEX TERMS Antenna, impedance matching, antenna tuner, radio transmitter, MIMO, control system.

I. INTRODUCTION

The characteristics of an antenna may be modified by the effects of the electromagnetic characteristics of the surroundings (EECS). For a portable wireless device, a cause of the EECS is the electromagnetic interaction between the antenna and a person holding the portable wireless device, often referred to as “user interaction”.

In current flagship mobile phone designs, automatic antenna tuning, which automatically adjusts a tunable passive antenna (TPA) and/or an antenna tuner (AT), has become increasingly prominent as a method to support the growing range of LTE or 5G frequencies, mitigate the EECS, reduce the size of the antennas, increase overall power efficiency and signal consistency, and obtain the highest possible data transmission rates [1]–[3]. Automatic antenna tuning is also common in land mobile, marine and tactical HF radio transceivers, as well as in radio transceivers for the amateur service [4]–[5].

This article is about control schemes which can be used, in a radio transceiver or radio transmitter, to automatically adjust an AT. Each AT shown in Fig. 1 has a port, referred to as “antenna port”, which is directly or indirectly coupled to an antenna, and another port, referred to as “radio port” (or as “user port”), for transmitting and/or receiving radio signals through the AT and the antenna. In the case of a transceiver using time-division duplex (TDD), each port may be an input port or an output port, depending on whether emission or reception is taking place. In the case of a transceiver using frequency-division duplex (FDD), both ports are input ports and output ports, simultaneously. The AT is linear with respect to its antenna port and radio port. Each AT shown

in Fig. 1 is a single-antenna-port (SAP) AT, but a multiple-antenna-port (MAP) AT may be needed for MIMO radio transmission.

Several authors have proposed descriptions of some SAP AT control schemes applicable to a transmitter, and defined categories [6]–[8]. Sections II to VIII provide a review of existing SAP AT control schemes for wireless transmitters, and a new classification into 5 types. Appendices A and B present a new analysis of their accuracy. In Section IX, we qualitatively compare the different types. Section X provides simulations of some properties of the different schemes, in a particular case.

Sections XI and XII cover the MAP AT control schemes for a radio transmitter using multiple antennas, including a new classification into 4 types. Appendix C explains some aspects of the signal processing used in these schemes, and Appendix D presents a new analysis of their accuracy.

II. DEFINITIONS AND ASSUMPTIONS

Several control schemes, which can be used to automatically adjust a SAP AT of a wireless transmitter, are based on one of the two configurations shown in Fig. 1. In both configurations, the transmitter comprises: an antenna; the AT; a sensing unit (SU); a control unit (CU); and a transmission and signal processing unit (TSPU) which consists of all parts of the transmitter not shown elsewhere in Fig. 1.

The TX port of the TSPU delivers an excitation which is a bandpass signal having a carrier frequency denoted by f_C . The SU delivers, to the TSPU, one or more sensing unit output signals determined by one or more electrical variables (such as voltage, current, incident or forward voltage, etc)

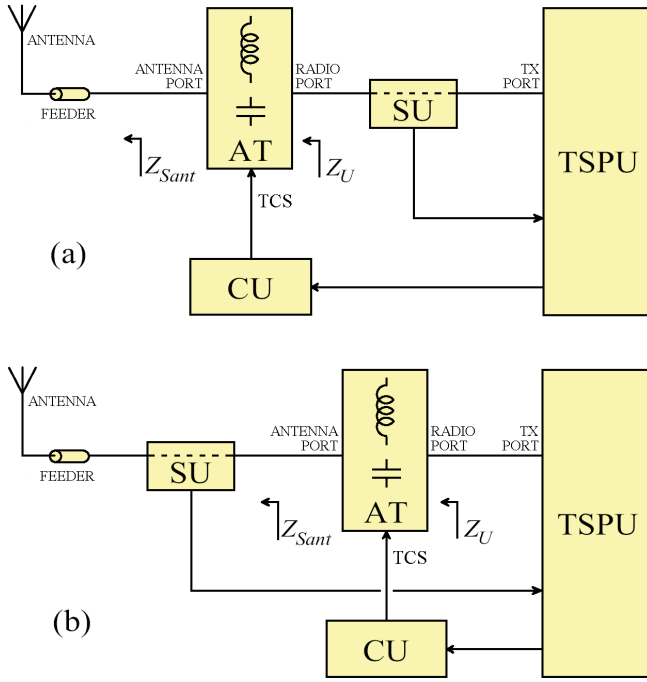


FIGURE 1. Two possible configurations of a transmitter comprising an antenna, a SAP antenna tuner (AT), a sensing unit (SU), a control unit (CU) and a transmission and signal processing unit (TSPU).

caused by the excitation, sensed at the radio port in the case of Fig. 1(a) or at the antenna port in the case of Fig. 1(b). The CU is an interface that delivers at least one tuning control signal (TCS) to the AT.

The AT comprises one or more adjustable impedance devices (AIDs) each having a reactance which is adjustable by electrical means. Adjusting an AT means adjusting the reactance of one or more of its AIDs. At a given time τ , a nominal reactance of an AID at f_C is determined by initial conditions of the AID at an earlier time τ_0 , and by the history of at least one TCS in the time interval $[\tau_0, \tau]$. The reactance and the resistance of the AID are functions of the nominal reactance of the AID and of other variables such as temperature, humidity, aging, uncertainties, etc. The resistance of the AID is unwanted because it entails an unwanted loss.

We identify 3 AID categories, each requiring particular TCSs. They may be defined as follows:

- category 1 refers to an AID in which controlled switches are used to obtain a finite number of nominal reactance values at f_C (e.g., an AID which is a network comprising capacitors or coils or open-circuited stubs or short-circuited stubs, and one or more electrically controlled switches or change-over switches, such as electro-mechanical relays, or MEMS switches, or PIN diodes, or insulated-gate FETs, used to cause different capacitors or coils or stubs of the network to contribute to the reactance [2], [9]);
- category 2 refers to an AID which does not belong to category 1, and such that, after a delay larger than the response time of the AID, its nominal reactance at f_C is mainly determined by the present value of at least

one TCS (e.g., an AID whose reactance is determined by one or more variable capacitance diodes, or barium strontium titanate (BST) varactors [2]);

- category 3 refers to an AID which neither belongs to category 1 nor to category 2 (e.g., an AID such as a motorized variable capacitor, a motorized variometer or a motorized roller inductor, in which the one or more TCSs applied to the motor cause a variation of the nominal reactance value at f_C [4]).

AIDs of categories 1 and 2 are commonly used in low-power applications (e.g., mobile phones). AIDs of categories 1 and 3 are commonly used in medium and high-power applications. Though AIDs of categories 1 and 2 often include non-linear components that may cause non-linear effects during emission, we assume that the AT behaves, with respect to its radio port and antenna port, substantially as a passive linear 2-port device.

We use Z_{Sant} to denote the impedance seen by the antenna port, and Z_U to denote the impedance presented by the radio port, which depends on Z_{Sant} and on the impedances of the AIDs. A wanted value of Z_U being denoted by Z_W , the user port tuning range, denoted by $D_{UTR}(Z_W)$, is the set of all Z_{Sant} for which there exist achievable values of the nominal reactances of the AIDs, such that $Z_U = Z_W$ at f_C [10].

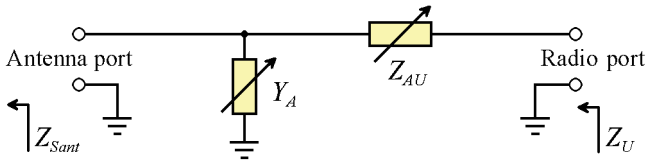
In the literature on ATs, “open-loop” often erroneously refers only to a control scheme without SU, so that the AT is typically adjusted only as a function of the operating frequency, which is known to the TSPU [2, Sec. 4.5.1], [11]. In this article, using the correct terminology, “open-loop control” means: control which does not utilize a measurement of the controlled variable [12].

In contrast, “closed-loop control” (which is also referred to as “feedback control”) means control in which the control action is made to depend on a measurement of the controlled variable [12]. This definition does not imply that the control action repetitively or continuously depends on a repetitive or continuous measurement of the controlled variable.

In what follows, “model-based” refers to a control scheme which uses a model that describes relevant properties of the AT and the CU, and which can use a single sample of each of the one or more sensing unit output signals to produce nominal AID reactance values intended to provide the wanted adjustment of the AT.

III. TYPE 0 CONTROL SCHEMES

Type 0 designates the open-loop AT control schemes which do not use any SU. In subtype *a* of type 0, the nominal reactance (or an equivalent variable) of each AID is determined only as a function of an operating frequency f_O , typically by utilizing a lookup table, the entries of which have for instance been determined based on experiments. In subtype *b*, the nominal reactance of at least one AID (or an equivalent variable) is determined as a function of an operating frequency f_O and of at least one auxiliary variable which is assumed to be correlated with some electromagnetic characteristics of the surroundings of the transmitter. In a


FIGURE 2. A SAP AT having an L-network structure.

mobile phone, such an auxiliary variable may for instance be [13]:

- a localization variable assumed to depend on a distance between a part of a human body and a zone of the transmitter, determined by a sensor such as a capacitive proximity sensor, an infrared proximity sensor, etc;
- a localization variable determined by a change of state of a switch of a keypad, or by a touchscreen;
- a communication type variable that indicates whether a radio communication session is a voice session or a data session; or
- a speakerphone mode activation indicator, etc.

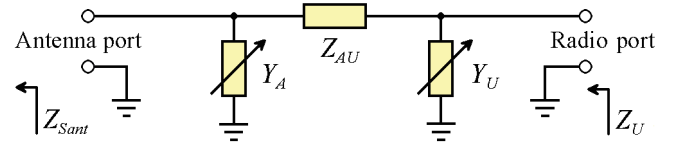
The idea of subtype *b* is that such auxiliary variables can be used to mitigate the EECS, statistically, if a correlation exists between f_O and the one or more auxiliary variables on the one part, and optimal nominal reactance values on the other part. In practice, the nominal reactance value (or the value of the equivalent variable) of each AID may be obtained from a lookup table, as a function of f_O and of a typical use configuration determined based on the one or more auxiliary variables.

IV. TYPE 1 SAP AT CONTROL SCHEMES

For a SAP AT, type 1 designates the control schemes which use the configuration of Fig. 1 (a) and are such that the TCSs are determined by a feedback control system which seeks to obtain a wanted value of Z_U at f_C , without implementing extremum-seeking control. The schemes using the configuration of Fig. 1 (a) and extremum-seeking control are the type 2 control schemes presented in Section V, in which a detailed definition of extremum-seeking control is provided.

In a type 1 control scheme, the TSPU estimates q real quantities depending on Z_U , where q is typically equal to two. We can identify 3 subtypes. Subtype *a* designates the schemes using continuous-time control, such as the ones described in [4], [7, Sec. IV-A], and [14]-[16]. Subtype *b* designates the non-model-based schemes which utilize discrete-time control, such as the schemes described in [7, Sec. IV-B] and [17]-[19]. Subtype *c* designates the model-based discrete-time control schemes, such as the ones described in [20]-[24].

Let Z_W be the wanted value of Z_U . In practice, a type 1 control scheme is designed for a particular SAP AT structure. For subtypes *a* and *b*, the reactance of each AID is typically determined by a separate feedback control loop which uses one of the q real quantities depending on Z_U as feedback signal. For instance, let us assume that the AT has the L-network structure shown in Fig. 2, in which the variable parallel admittance Y_A and the variable series impedance


FIGURE 3. An AT having a π -network structure.

Z_{AU} each correspond to an AID [25]. If we ignore losses in the AT, we have, at the frequency f_C ,

$$Z_U = \frac{1}{\frac{1}{Z_{Sant}} + jB_A} + jX_{AU}, \quad (1)$$

where the real susceptance B_A and the real reactance X_{AU} are such that $Y_A = jB_A$ and $Z_{AU} = jX_{AU}$. Let us assume that Z_W is real. Since $\partial Z_U / \partial X_{AU} = j$, an inner feedback loop using $\text{Im}(Z_U)$ or $\arg(Z_U)$ as feedback signal may easily be designed to control Z_{AU} and provide a zero $\text{Im}(Z_U)$. At the frequency f_C and ignoring losses in the AT, we have

$$\text{Re}(Z_U) = \frac{G_{Sant}}{G_{Sant}^2 + (B_{Sant} + B_A)^2}, \quad (2)$$

where the real conductance G_{Sant} and the real susceptance B_{Sant} are such that $G_{Sant} + jB_{Sant} = 1/Z_{Sant}$. It follows that $Z_U = Z_W$ is possible only if $\text{Re}(Z_W) \leq 1/G_{Sant}$, and that

$$\frac{\partial \text{Re}(Z_U)}{\partial B_A} = \frac{-2G_{Sant}(B_{Sant} + B_A)}{[G_{Sant}^2 + (B_{Sant} + B_A)^2]^2}. \quad (3)$$

Thus, if the antenna and the AIDs are such that the sign of $B_{Sant} + B_A$ is known by design, an outer feedback loop using $k\text{Re}(Z_U)$, where k is real, as feedback signal may be designed to control Y_A and provide $\text{Re}(Z_U) = \text{Re}(Z_W) = Z_W$. Also, if the outer feedback loop is made much slower than the inner feedback loop, $k|Z_U|$ may be used as a feedback signal of the outer feedback loop.

If the sign of $B_{Sant} + B_A$ is not known, a stable subtype *a* or *b* control scheme is more difficult to design for the AT shown in Fig. 2. For instance, a possible route would be to ensure that, when the control system is switched on, $B_{Sant} + B_A$ has always the wanted sign, so that this sign would be maintained thereafter by the feedback control system, provided B_{Sant} and f_C never vary too rapidly, and provided Z_{Sant} remains in or close to the user port tuning range $D_{UTR}(Z_W)$ of the AT at f_C .

Let us now consider a subtype *a* or *b* control scheme using the AT shown in Fig. 3, which has a π -network structure [25]-[26]. Here, the series impedance Z_{AU} is fixed, and the variable parallel admittances Y_A and Y_B each correspond to an AID. If we ignore losses in the AT, we have, at the frequency f_C ,

$$\frac{1}{Z_U} = \frac{1}{\frac{1}{\frac{1}{Z_{Sant}} + jB_A} + jX_{AU}} + jB_U, \quad (4)$$

where the real susceptance B_U is such that $Y_U = jB_U$. Since $\partial(1/Z_U)/\partial B_U = j$, an inner feedback loop using $\text{Im}(1/Z_U)$ or $\text{Im}(Z_U)$ or $\arg(Z_U)$ as feedback signal may be designed to control Y_U and provide a zero $\text{Im}(1/Z_U)$. However, the reader can easily check that $\partial(1/Z_U)/\partial B_A$ and $\partial Z_U/\partial B_A$ are involved, so that a stable subtype a or b control scheme is difficult to design for the AT shown in Fig. 3.

The error of a subtype b control scheme is determined in subsection B of Appendix A.

For subtype c , the control scheme is based on a model of the SAP AT and of the CU. For instance, let us assume that the AT is the one shown in Fig. 3, that the nominal reactance of any one of the AIDs is determined by a tuning unit adjustment instruction received by the CU, and that the absolute value and the phase of Z_U have been estimated, at f_C , for nominal AID reactances determined by an initial tuning unit adjustment instruction [23]-[24]. In a first step, the TSPU estimates Y_A , Z_{AU} and Y_U using the model and the initial tuning unit adjustment instruction, and then Z_{Sant} using

$$\frac{1}{Z_{Sant}} = \frac{1}{\frac{1}{\frac{1}{Z_U} - Y_U} - Z_{AU}} - Y_A. \quad (5)$$

If the estimated Z_{Sant} lies in or close to the user port tuning range $D_{UTR}(Z_W)$ of the AT at f_C , the TSPU can, in a second step, compute a subsequent tuning unit adjustment instruction such that, according to the model, Z_U at f_C is close to Z_W . This computation may for instance use the fast algorithm proposed in [27, Appendix C], which takes losses in the AT into account. The operation of the control system may stop at this point, so that the nominal AID reactances directly jump from the ones determined by the initial tuning unit adjustment instruction, to the ones determined by the subsequent tuning unit adjustment instruction, by utilizing the model twice. The error of a subtype c control scheme, at the end of the adjustment sequence that we have just described, is determined in subsection E of Appendix A.

If the model of the AT and of the CU is not accurate, the subsequent tuning unit adjustment instruction may produce a Z_U at f_C which is not close to Z_W . In subsection F of Appendix A, it is shown that, in this case, repeating the steps that we have just described typically reduces the error of the subtype c control scheme, and makes the error almost independent of the accuracy of the model.

In practice, one or more lookup tables are needed to obtain an accurate model. Additionally, some of the computations can be replaced with interpolations, if a suitable lookup table, or a suitable set of lookup tables, is provided.

For AIDs of category 1, subtype b control schemes using digital processing or subtype c control schemes are preferred.

V. TYPE 2 SAP AT CONTROL SCHEMES

For a SAP AT, type 2 designates the control schemes which use the configuration of Fig. 1 (a) and in which the TSPU uses extremum-seeking control to obtain that Z_U at f_C approximates a wanted value Z_W .

Extremum-seeking control is a family of nonlinear control methods whose purpose is to autonomously find either a maximum or a minimum of a performance variable which is a real function of one or more outputs of a controlled system, by controlling one or more inputs of the controlled system. In an extremum-seeking control algorithm, one or more signals varying over time are caused to appear at these one or more inputs of the controlled system, in a way that allows the algorithm to probe the nonlinearity of the performance variable with respect to the one or more inputs of the controlled system, and to get closer to an extremum. Thus, extremum-seeking control algorithms are based on the information that the extremum exists, but they do not need an exact knowledge of the controlled system to find the extremum. For this reason, extremum seeking control is said to be a non-model-based real-time optimization approach. A type of extremum-seeking control which uses one or more periodical perturbations is usually referred to as perturbation based extremum-seeking control [28]. There are many other types of extremum-seeking control, such as sliding mode extremum-seeking control, neural network extremum-seeking control, relay extremum seeking control, perturb and observe, numerical optimization based extremum-seeking control, stochastic extremum-seeking control, etc [29]-[31].

In an automatic AT control scheme, the nominal reactances of the one or more AIDs may be regarded as the “one or more inputs of the controlled system”. Thus, the extremum-seeking control algorithm controls and varies the AID reactances over time, to get closer to an extremum of the performance variable.

The performance variable may be substantially the absolute value of the reflection coefficient at the radio port, or any monotone function of this quantity [31, ch. 7], [32]-[35]. The absolute value of this reflection coefficient is a performance variable which typically varies very little far from the sought global minimum, and which may present several local minima at a given frequency. Thus, a type 2 control scheme must be designed to avoid that the extremum-seeking control algorithm fails to converge, or converges to a local extremum which is not the wanted global extremum. For this reason, in a typical type 2 control scheme, suitable initial values of the nominal AID reactances are generated before extremum seeking starts, as a function of f_C , using one of the type 0 control schemes.

We define 2 subtypes. Subtype a designates the schemes using continuous-time extremum-seeking [28]. Subtype b designates the schemes using discrete-time extremum-seeking, such as the ones described in [32]-[35]. For subtype b , the error is computed in subsection B of Appendix A.

It is worth mentioning that subtype b includes a brute force extremum seeking technique applicable to the case where each AID can provide a finite (and small) number of nominal reactance values: all combinations of AID reactance values are tested, and a combination providing either the larger or the smaller value of the performance variable is selected [36]-[38]. This approach does not use initial values of the nominal AID reactances determined as a function of f_C .

VI. TYPE 3 SAP AT CONTROL SCHEMES

For a SAP AT, type 3 designates the model-based control schemes which use the configuration of Fig. 1(b) and are such that: the TSPU estimates q real quantities depending on Z_{Sant} at f_C ; and the nominal reactance (or an equivalent variable) of at least one AID is determined as a function of f_C and of these real quantities, using a model of the AT and of the CU. Typically, $q = 2$ [39]-[40]. Since type 3 is an open-loop control scheme, an accurate knowledge of the characteristics of the AT is essential for good results. If these characteristics depend on temperature, it is advantageous to take into account one or more temperatures in the AT to determine the TCSs [41]. The aim of a type 3 control scheme is unconstrained, that is to say: it may be arbitrarily defined.

If the aim of the control scheme is to obtain a wanted value Z_W of Z_U at f_C , we observe that the type 3 control scheme has much in common with the second step of the operation of a type 1 subtype c control scheme, presented above in Section IV. For instance, in the case of an AT having the structure of a π -network, suitable TCSs may be determined using the iterative computation technique of [27, Appendix C], or a numerical algorithm that minimizes a suitable performance variable, for instance $|Z_U - Z_W|^2$ computed using the model of the AT and of the CU. A detailed algorithm which directly takes into account the set of the nominal reactance values of the AIDs has been disclosed [42].

If the aim of the control scheme is to maximize the average power delivered by the antenna port at f_C , denoted by P_{Sant} , suitable TCSs may be determined using a numerical algorithm that maximizes P_{Sant} computed using the model of the AT and of the CU.

The error of a type 3 control scheme is determined in subsection D of Appendix A, or in Appendix B, according to the aim. This error depends on the accuracy of the model.

For any aim of the control scheme, some or all of the computations can be replaced with interpolations, if a suitable lookup table is provided.

VII. TYPE 4 SAP AT CONTROL SCHEMES

For a SAP AT, type 4 designates the control schemes using the configuration of Fig. 1 (b) and such that [43]-[44]:

- an initial value of each nominal AID reactance is generated, using open-loop control; and
- to increase as much as possible the average power delivered by the antenna port at f_C , denoted by P_{Sant} , one or more subsequent values of one or more of the nominal AID reactances are generated, using an extremum-seeking control algorithm.

Generating initial nominal AID reactance values which are not too far from the one that would maximize P_{Sant} has two advantages: it avoids that the extremum-seeking control algorithm converges to a local extremum which is not the wanted global extremum, and it speeds up the convergence, for a given accuracy. For subtype a , the initial nominal AID reactance values are obtained as a function of f_C , using one of the type 0 control schemes. For subtype b , the initial nominal AID reactance values are obtained as a function of

f_C and of one or more real quantities depending on Z_{Sant} , using a type 3 control scheme.

The extremum-seeking control algorithm seeks to maximize or to minimize a performance variable estimated as a function of one or more sensing unit output signals. To discuss possible performance variables, let $s_E(t)$ be the complex envelope of the excitation delivered by the TX port, $s_A(t)$ be the complex envelope of an electrical variable (e.g., a voltage, a current, an incident voltage, etc) sensed at the antenna port, and f be a function which is differentiable and strictly monotone over the set of positive real numbers.

If the excitation is not amplitude modulated, that is to say if $|s_E(t)|$ is constant, it is easily seen that a possible performance variable is $f(|s_A(t)|)$. For instance, if f is an increasing function, maximizing $f(|s_A(t)|)$ clearly maximizes P_{Sant} [45]-[47].

If the excitation is amplitude modulated, this approach does not work, because a variation in $|s_E(t)|$ creates a variation in $f(|s_A(t)|)$. In this case, we observe that, for given values of Z_{Sant} and of the AID reactances, $s_E(t)$ is substantially proportional to a modulating signal $s_M(t)$, so that $|s_A(t)|$ is substantially equal to $\lambda|s_M(t)|$, where λ is a positive real which we want to maximize. Here, a possible performance variable is $f(|s_A(t)|)/f(|s_M(t)|)$, provided f is such that, for any positive λ , the ratio $f(\lambda|s_M(t)|)/f(|s_M(t)|)$ is independent of $|s_M(t)|$. The function f must therefore be such that, for any positive λ and for any positive x , we have

$$\frac{f(\lambda x)}{f(x)} = \frac{f(\lambda)}{f(1)}. \quad (6)$$

Thus, we have

$$f(\lambda x) = \frac{f(x)f(\lambda)}{f(1)}. \quad (7)$$

Taking a partial derivative of (7) with respect to x , and a partial derivative of (7) with respect to λ , we obtain

$$\frac{f'(x)f(\lambda)}{\lambda f(1)} = \frac{f(x)f'(\lambda)}{x f(1)}, \quad (8)$$

in which f' is the derivative of f . For $\lambda = 1$, we obtain the differential equation

$$\frac{f'(x)}{f(x)} = \frac{1}{x} \frac{f'(1)}{f(1)}. \quad (9)$$

This is not a linear differential equation. However, if we first consider that $k = f'(1)/f(1)$ is an arbitrary variable, we can integrate the resulting first-order linear differential equation of parameter k . This allows us to find that the solutions of (9) are the functions which satisfy

$$f(x) = K x^k, \quad (10)$$

where k and K are real constants, K being nonzero. Conversely, all functions given by (10) satisfy (6), and are strictly monotone for k nonzero. Thus, for an amplitude modulated excitation, the suitable functions f are given by (10) where k and K are nonzero real constants.

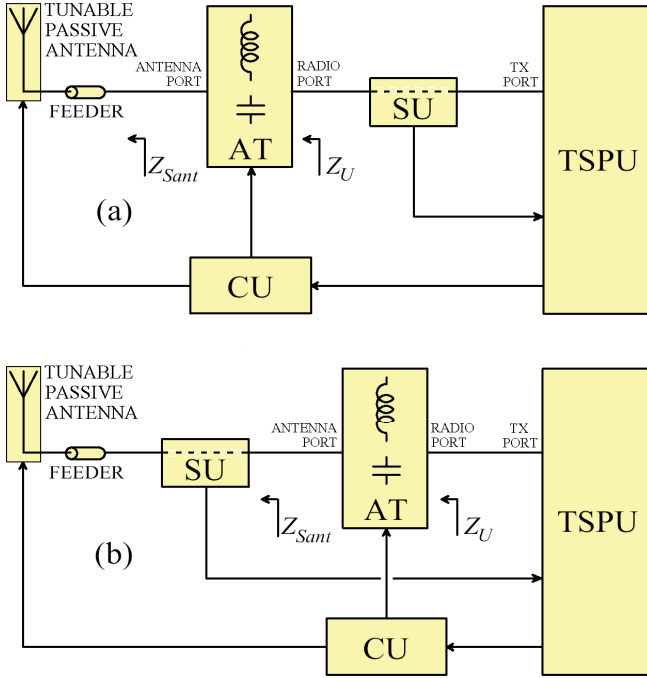


FIGURE 4. Two possible configurations of a transmitter comprising a tunable passive antenna (TPA), a SAP antenna tuner (AT), a sensing unit (SU), a control unit (CU) and a transmission and signal processing unit (TSPU).

Ideally, a type 4 control scheme maximizes P_{Sant} with respect to the reactances of the AIDs. This maximization does not entail conjugate matching at the antenna port (as opposed to a maximization of P_{Sant} with respect to the resistance and the reactance seen by the antenna port). The error of the control scheme is determined in Appendix B.

If the radio port sees a linear source of impedance Z_S , an ideal type 4 control scheme maximizes the transducer power gain of the AT at f_C . If the AT is a part of a transceiver using TDD, what was said above applies to emission. If we further assume that the AT is reciprocal with respect to its radio port and antenna port, and that the radio port sees a linear load of impedance Z_S during reception, then the AT adjustment obtained for emission maximizes the transducer power gain of the AT during reception. This follows from a well-known reciprocal power theorem [48, Sec. IV], according to which the transducer power gain of the AT during reception is equal to the transducer power gain of the AT during emission.

VIII. OTHER SAP AT CONTROL SCHEMES

We have defined five types of control scheme which can be used to automatically adjust a SAP AT of a radio transmitter. They cover most schemes described in the literature, but not all of them.

First, some AT control schemes use more than one SU, for instance: one SU at the radio port and one SU inside the AT [8], [49]; or one SU at the radio port and another one at the antenna port [50]-[51]. Many variations are possible.

Second, an AT may be used in conjunction with a tunable passive antenna (TPA), also referred to as “reconfigurable antenna”, which may be a frequency-agile antenna [52]. This

combination, shown in Fig. 4, can provide a broader tuning range than the one provided by the AT alone, and reduced feeder losses [53]-[57]. An adjustment of a TPA may provide a change in its directivity pattern, and/or a change in its impedance. If the TPA is such that adjusting it produces a change in its impedance, an automatic control system may use the adjustment of the TPA to obtain a coarse adjustment of Z_{Sant} , and then use the AT to obtain a fine adjustment, using any type of control scheme.

Here, it is worth noting that some authors strangely refer to the adjustment of a TPA as “aperture tuning”, and to the adjustment of an AT as “impedance tuning”.

IX. COMPARISON OF SAP AT CONTROL SCHEMES

A. CLOSED-LOOP VERSUS OPEN-LOOP

Since an extremum-seeking control algorithm is based on closed-loop control, we can say that types 1, 2 and 4 utilize closed-loop control, whereas type 0 and type 3 only utilize open-loop control. A remarkable characteristic of a typical AT control system is the severe non-linearity of the equations that govern the AT, for instance visible in (1)-(4). The relation between the reactance of an AID and the TCS(s) it receives is typically also involved. For these reasons, a continuous-time (analog) closed-loop control system, if started far from its goal, is typically unable to reach it, or to reach it in a reasonable time. Consequently, we may assume that practical type 1 and type 2 control schemes include a preliminary open-loop step, of type 0. Type 4 always includes a preliminary open-loop step, of type 0 or type 3. Thus, most current closed-loop control designs use digital circuits and lookup tables, because they are unavoidable for an open-loop control step; and closed-loop control systems without digital circuits (which can only be of type 1 subtype *a* or type 2 subtype *a*) are outdated for most applications.

B. MEASUREMENTS AND MITIGATION OF EECS

The requirements on the SU and the processing of sensing unit output signals depend on the control scheme, as shown in Table 1. The easiest measurements are: the scalar reflection coefficient measurements at the radio port, used in type 2, which need only be accurate in the vicinity of $Z_U = Z_W$ if an effective preliminary open-loop step has been used; and the scalar measurements at the antenna port, used in type 4 subtype *a*, which can be relative voltage or current measurements, since they are only used to find a maximum power. Vector impedance measurements at the radio port, used in type 1, are more involved, but they need only be accurate in the vicinity of $Z_U = Z_W$ if an effective preliminary open-loop step has been used. Vector impedance measurements at the antenna port, used in type 3 and type 4 subtype *b*, are the most challenging, because accuracy is needed in the entire set of possible values of Z_{Sant} .

As shown in Table 1, mitigation of the EECS is obtained for all schemes using a SU, that is to say, for all schemes except type 0. A scheme that can mitigate the EECS can also compensate other causes of antenna performance degradation: manufacturing tolerances, aging, temperature, etc.

TABLE 1. Some possible characteristics of the SAP AT control scheme types and subtypes defined in Section III to Section VII.

Type	Figure	Subtype	Measurement	Mitigation of EECS	Aim of control	Accuracy	Speed
0	-	<i>a</i>	none	no	any	poor	very fast
		<i>b</i>	auxiliary variable	limited	any	poor	very fast
1	1(a)	<i>a</i>	vector at radio port	yes	$Z_U = Z_W$	very good	slow / fast
		<i>b</i>	vector at radio port	yes	$Z_U = Z_W$	very good	fast
		<i>c</i>	vector at radio port	yes	$Z_U = Z_W$	good / very good	very fast / fast
2	1(a)	<i>a</i>	scalar at radio port	yes	$Z_U = Z_W$	very good	very slow / medium
		<i>b</i>	scalar at radio port	yes	$Z_U = Z_W$	very good	medium
3	1(b)	-	vector at antenna port	yes	any	good	very fast
4	1(b)	<i>a</i>	scalar at antenna port	yes	maximizing P_{Sant}	very good	medium
		<i>b</i>	vector at antenna port	yes	maximizing P_{Sant}	good / very good	very fast / fast

C. AIM OF THE CONTROL SCHEME AND DESIGN GOAL

The aims of the different control schemes are shown in Table 1. How do these aims correspond to possible design goals?

Let us for a while assume that the design goal is a maximization of P_{Sant} , in a context where the TX port of the TSPU need not be linear, and where the SU is transparent to the signals intended for the antenna. In the case of a lossless AT, the average power delivered by the TX port is equal to P_{Sant} , so that a maximum power delivered by the TX port corresponds to a maximum P_{Sant} (if the TX port was linear, a maximum power delivered by the TX port would imply a conjugate matching at the TX port). Thus, in the case of a lossless AT, a type 1, 2 or 3 control scheme, configured to provide a value of Z_U which maximizes the power delivered by the TX port at f_C (we assume that this value is known), maximizes P_{Sant} , like a type 4 control scheme. If losses in the AT are not very small, a maximum power delivered by the TX port need not correspond to a maximum P_{Sant} , so that the types 1, 2 and 3 control schemes considered above are not optimal for the design goal, while type 4 is optimal. It is advisable to investigate if the degradation in P_{Sant} inherent to a type 1, 2 or 3 control scheme can be ignored.

The possible maximization of the transducer power gain during TDD reception, explained in Section VII, is another advantage of type 4.

Let us now assume that the design goal is $Z_U = Z_W$, for instance because it provides a wanted linearity or spectral purity, or a wanted efficiency of a power amplifier, or simply because Z_W is the nominal load of the TX port. Here, a type 1, 2 or 3 control scheme can be optimal, if it is configured to provide $Z_U = Z_W$, while type 4 is not optimal (except in the case of a lossless AT). This may require an investigation.

D. ACCURACY, SPEED AND DEPENDENCE ON A MODEL OF THE AT

The performance of a control system depends on many implementation details. However, as a guideline, Table 1 indicates the relative accuracy and speed of the different

control systems, based on the following considerations:

- all schemes using only open-loop control are very fast, but cannot be very accurate, because their accuracy depends on a model of the AT, and models are imperfect;
- all schemes using closed-loop control are very accurate, but type 1 subtype *c* is special, because it is very accurate if used with a sufficient number of repetitions, but has a reduced accuracy if used without repetition;
- the schemes using closed-loop discrete-time control are supposed to include a preliminary open-loop step, so that the characteristics of the open-loop and closed-loop steps interact to provide accuracy and speed;
- if they do not include a preliminary open-loop step, the schemes using closed-loop continuous-time control (type 1 subtype *a* and type 2 subtype *a*) are slow at best; in the opposite case, their speed is similar to the one of the discrete-time control scheme of same type;
- all schemes using closed-loop control are significantly slower than an open-loop scheme, but type 1 subtype *c* and type 4 subtype *b* are special, the latter because it includes an accurate and very fast preliminary type 3 step, so that a value of P_{Sant} which is very close to the aimed maximum value is obtained very quickly;
- type 2 subtype *a* is slower than type 1 subtype *a*, and type 2 subtype *b* is slower than type 1 subtype *b*, because in type 2 schemes, a non-model-based extremum-seeking control algorithm must probe the non-linearity of the performance variable, so that it follows an indirect path toward its aim.

The model-based control schemes are type 1 subtype *c*, type 3 and type 4 subtype *b*. The subtypes *a* and *b* of type 1 are not model-based, even though they use a model of the AT to determine in which direction the nominal reactance of each AID must vary, in order to move from the current value of Z_U toward Z_W . Model-based control schemes are very fast but computationally demanding, in particular type 1 subtype *c* because it uses the model twice, at least, in an adjustment sequence.

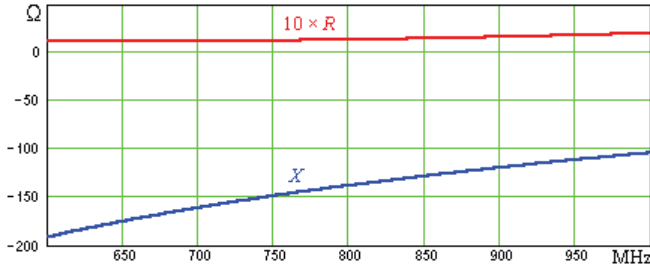


FIGURE 5. Real part R and imaginary part X of the impedance Z_{Sant} seen by the antenna port, for $d = 0.1$ m.

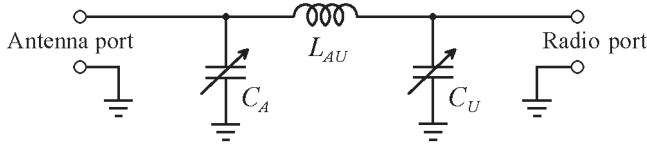


FIGURE 6. An AT having a π -network structure.

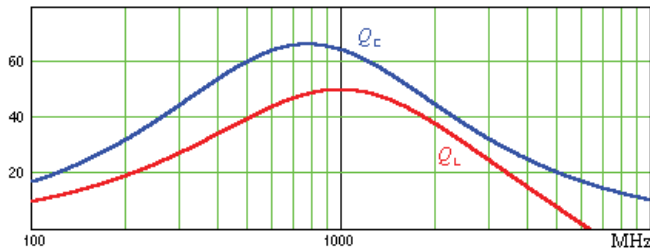


FIGURE 7. Quality factor Q_L of the coil and quality factor Q_C of each adjustable impedance device, for the AT of Section X.

X. EXAMPLE FOR A QUANTITATIVE COMPARISON

We now want to illustrate the qualitative comparison of Section IX with simulation results suitable for a quantitative comparison of SAP AT control schemes.

We are going to investigate several SAP AT control schemes, implemented on a theoretical system comprising a 74.9-mm-long dipole antenna, used in the frequency range 600 MHz to 1 GHz, a lossy feeder, and the AT shown in Fig. 6, which consists of a coil of inductance L_{AU} and two AIDs each presenting a negative reactance, of capacitances C_A and C_U , respectively. The configuration also includes a large plate made of a perfect electrical conductor (PEC) lying parallel to the antenna, at a distance d of the antenna, used to create and vary the EECS. The impedance Z_{Sant} presented by the antenna and the feeder varies as a function of the frequency and of d . The computed values of Z_{Sant} for $d = 0.1$ m are shown in Fig. 5.

We clearly have an electrically small antenna with a small radiation power factor R/X , for which an impedance matching network can provide a match to an arbitrary resistance, but only over a narrow bandwidth [58].

The antenna and PEC are physically realizable, but not meant to represent an actual use configuration. However, they are suitable for our purpose, and allow the reader to easily reproduce our results. In contrast, our model of the AT is representative of what can be achieved in a hand-held transceiver. For L_{AU} , we use the coil model presented in [27,

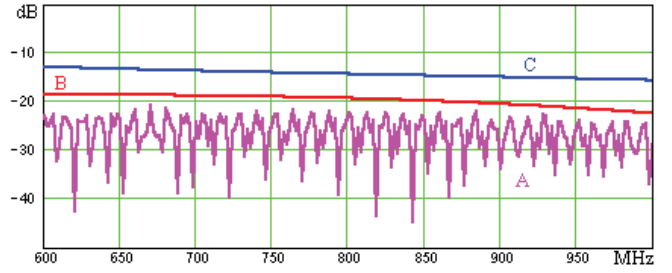


FIGURE 8. Reflection coefficient at the radio port versus frequency, for $d = 0.1$ m. Curve A: effect of discretization on type 1, 2 or 3. Curve B: worst case of type 3 with 1% uncertainty. Curve C: type 4.

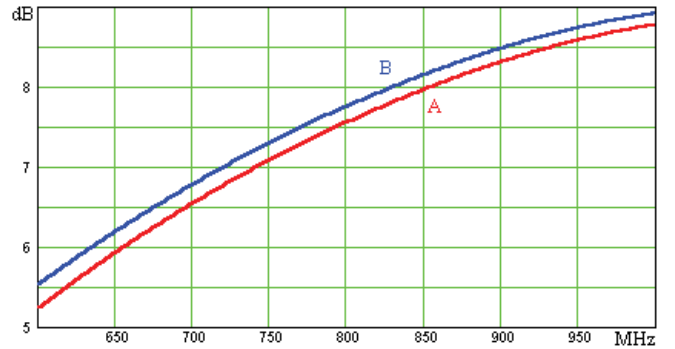


FIGURE 9. Insertion gain versus frequency, for $d = 0.1$ m. Curve A: type 1, type 2 or type 3 using an accurate AT model. Curve B: type 4.

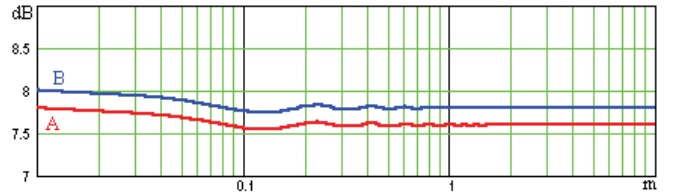


FIGURE 10. Insertion gain versus d , at 800 MHz. Curve A: type 1, type 2 or type 3 using an accurate AT model. Curve B: type 4.

Sec. 5], with $L_N = 10$ nH, $R_S \simeq 641$ m Ω , $R_P \simeq 6.74$ k Ω and $C \simeq 63.4$ fF. Fig. 7 shows the quality factor Q_L of the coil. For C_A and C_U , we use the AID model of [27, Sec. 5], with $\omega_P = 37 \times 10^6$ rd/s and $\omega_S = 650 \times 10^9$ rd/s. According to this model, the quality factor is independent of the capacitance value. Fig. 7 shows the quality factor Q_C of the AIDs. We also assume accurate sensing unit output signals, and an accurate analog or digital signal processing.

We say that an AID is continuously adjustable (CA) if its set of nominal reactance values is an interval. Types 1 and 2 can exactly provide $Z_U = Z_W$, if each AID is CA. The same applies to a type 3 control scheme aiming $Z_U = Z_W$, if, in addition, it uses an exact model of the AT. In Fig. 8, we assume $Z_W = 50$ Ω , and we show the reflection coefficient at the radio port, defined with respect to Z_W , after automatic adjustment of the AT, in some cases which do not exactly provide $Z_U = Z_W$. For types 1, 2 and 3 control schemes using AIDs which are not CA, Fig. 8(A) shows the effect of a discretization of the capacitance values (64 logarithmically spaced nominal values for C_A and C_U). For type 3 and CA AIDs, Fig. 8 (B) shows the effect of an inaccurate AT model

(1% uncertainty of the nominal values for C_A and C_U). The results for type 4 and CA AIDs are shown in Fig. 8 (C).

In Fig. 9 and Fig. 10, we assume that the TX port is linear and presents an impedance of 50Ω , we assume continuous AIDs, and we show the insertion gain of the AT, i.e., the ratio of the power delivered by the antenna port of the automatically adjusted AT, to the power received by the feeder if it was directly coupled to the TX port. For type 3, we also assume an exact model of the AT. Type 4 maximizing the power delivered by the antenna port, the plots show that type 1, 2 and 3 are not optimal, by an amount ranging from about 0.14 dB to 0.29 dB in this example.

For type 4, the maximum reflection coefficient shown in curve C of Fig. 8 is about -12.9 dB, corresponding to a VSWR of about 1.58. The power amplifier of a typical transmitter operates without problem with a VSWR less than 2. If this applies to our transmitter, a type 4 control scheme can be used, and provides a more efficient transmitter than the other types, as shown in Fig. 9 and Fig. 10.

XI. CONTROL SCHEMES FOR MULTIPLE-ANTENNA-PORT ANTENNA TUNERS

A. NEW DEFINITIONS AND ASSUMPTIONS

We will now look at the control schemes which can be used to automatically adjust a multiple-antenna-port (MAP) AT of a transmitter using any number $n \geq 2$ of antennas simultaneously in the same frequency band, for instance for MIMO radio transmission.

A MAP AT has n antenna ports, each of which is directly or indirectly coupled to an antenna, and m radio ports (or “user ports”), for transmitting and/or receiving radio signals through the AT and the antennas. The AT is linear with respect to its antenna ports and radio ports. A MAP AT may be used to adjust the impedance matrix presented by the radio ports, denoted by \mathbf{Z}_U , so that it approximates a wanted impedance matrix \mathbf{Z}_W . Typically, \mathbf{Z}_W is a diagonal matrix because, if \mathbf{Z}_U is diagonal, it follows that:

- the radio ports are uncoupled, and therefore suitable for maximum power transfer from m uncoupled power amplifier outputs [59];
- there is no power amplifier performance degradation caused by active load modulation resulting from mutually coupled signals [60]-[62]; and
- if losses are sufficiently small, the radio ports have orthogonal radiation patterns, suitable for maximum capacity [63]-[66].

Two possible configurations of a wireless transmitter comprising a MAP AT such that $n = m = 2$ are shown in Fig. 11. A radio transmitter, which uses any number $n \geq 2$ of antennas simultaneously in the same frequency band, and which can automatically adjust a MAP AT, may be composed of: the antennas; the MAP AT; sensing units (SUs); a control unit (CU); and a transmission and signal processing unit (TSPU) which consists of all other parts of the transmitter. Several possible control schemes are based either on a configuration in which the SUs are coupled to the m radio ports, shown in Fig. 11(a) for $n = m = 2$, or on a

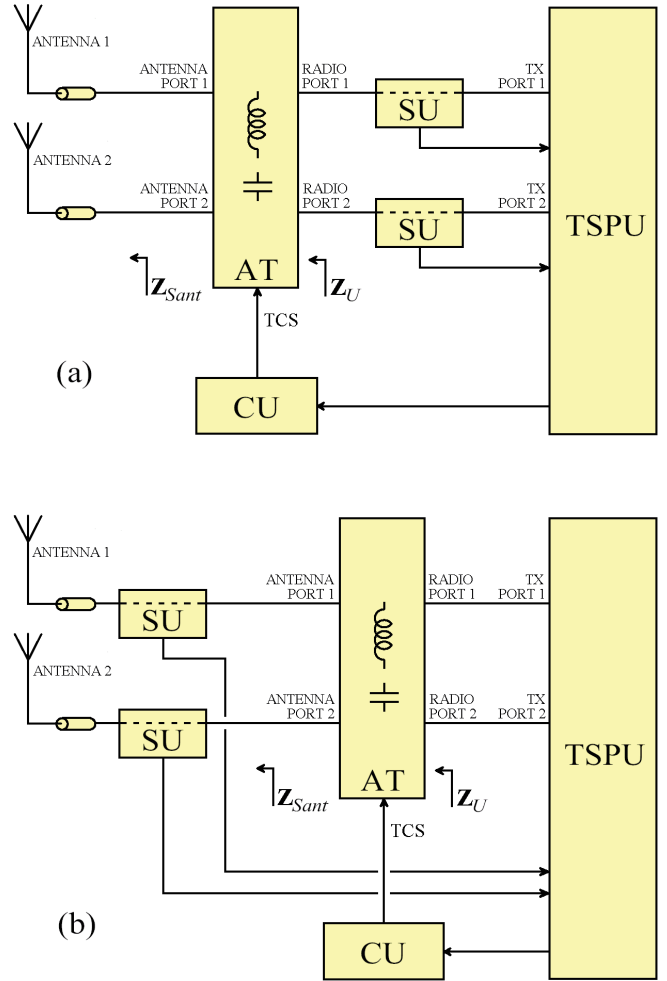


FIGURE 11. Two possible configurations of a transmitter comprising 2 antennas, a MAP antenna tuner (AT) having 2 antenna ports and 2 radio ports, 2 sensing units (SU), a control unit (CU) and a transmission and signal processing unit (TSPU).

configuration in which the SUs are coupled to the n antenna ports, shown in Fig. 11(b) for $n = m = 2$. The m TX ports of the TSPU deliver excitations which are bandpass signals having a common carrier frequency denoted by f_C . The SUs deliver, to the TSPU, sensing unit output signals determined by electrical variables caused by the excitations, sensed at the m radio ports or at the n antenna ports. The CU is an interface that delivers tuning control signals (TCSs) to the AT.

B. ABOUT THE MAP AT

The MAP AT comprises AIDs each having a reactance which is adjustable by electrical means, and adjusting the AT means adjusting the reactance of one or more of its AIDs. Let \mathbf{Z}_{Sant} be the impedance matrix seen by the antenna ports. \mathbf{Z}_U depends on \mathbf{Z}_{Sant} and on the impedances of the AIDs. If \mathbf{Z}_{Sant} is symmetric (i.e., the antennas are reciprocal), an AT which is reciprocal with respect to its radio ports and antenna ports is said to have a full tuning capability if [10]:

- any small symmetric variation $\delta\mathbf{Z}_U$ in \mathbf{Z}_U can be obtained, if suitable achievable values of the reactances of the AIDs exist; and

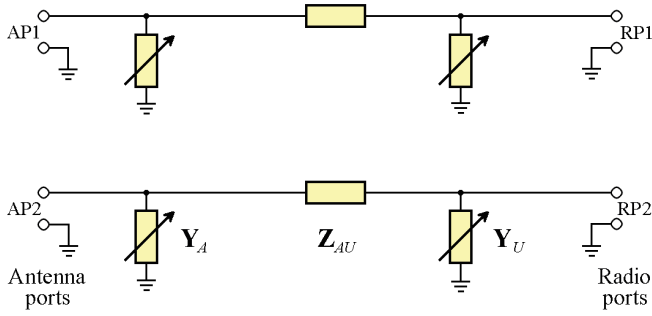


FIGURE 12. A MAP AT having $n = 2$ antenna ports (denoted by AP1 and AP2) and $m = 2$ radio ports (denoted by RP1 and RP2). This AT is made of 2 uncoupled π -networks.

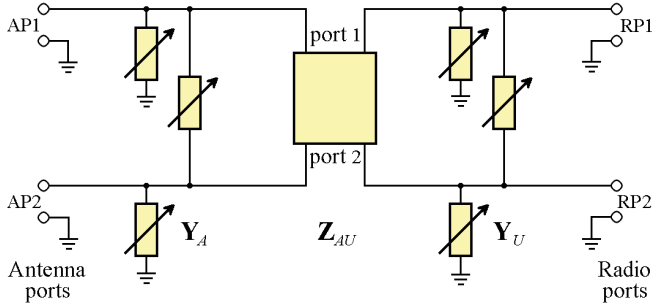


FIGURE 13. A MAP AT having $n = 2$ antenna ports (denoted by AP1 and AP2) and $m = 2$ radio ports (denoted by RP1 and RP2). This AT has the structure of a multidimensional π -network.

- any small symmetric variation $\delta\mathbf{Z}_{Sant}$ in \mathbf{Z}_{Sant} can be compensated to the first order in $\|\delta\mathbf{Z}_{Sant}\|$, if suitable achievable values of the reactances of the AIDs exist.

Let p be the number of AIDs in the AT. To obtain a full tuning capability, it is necessary that $p \geq m(m+1)$, but this condition is not sufficient [10].

A MAP AT may consist of uncoupled SAP ATs, one for each antenna [67]. For $m = n = 2$, an example of such a MAP AT, made of 2 uncoupled π -networks, is shown in Fig. 12. A MAP AT consisting of n uncoupled SAP ATs need not be able to provide a \mathbf{Z}_U that approximates \mathbf{Z}_W because, for $n \geq 3$, a MAP AT made of n uncoupled SAP ATs does not have a full tuning capability [10], [68]. However, interesting results may be obtained with this kind of MAP AT [69]-[74].

Recently, several MAP ATs which cannot be separated into uncoupled SAP ATs have been proposed and investigated [10], [27], [68], [75]-[80]. For $m = n = 2$, an example of such a MAP AT, having the structure of a multidimensional π -networks, is shown in Fig. 13. Such a MAP AT may be able to provide a \mathbf{Z}_U that approximates an arbitrary \mathbf{Z}_W .

The MAP ATs of Fig. 12 and Fig. 13 are both such that, at the frequency f_C ,

$$\mathbf{Z}_U = (((\mathbf{Z}_{Sant}^{-1} + \mathbf{Y}_A)^{-1} + \mathbf{Z}_{AU})^{-1} + \mathbf{Y}_U)^{-1}, \quad (11)$$

where \mathbf{Y}_A is the admittance matrix of the AIDs coupled in parallel with the antenna ports, where \mathbf{Z}_{AU} is an impedance matrix of the device(s) connected to a terminal of an antenna port and to a terminal of a radio port, and where \mathbf{Y}_U is the

admittance matrix of the AIDs coupled in parallel with the radio ports.

Though (11) is applicable to both of them, the two ATs produce different results, because \mathbf{Y}_A , \mathbf{Z}_{AU} , and \mathbf{Y}_U are diagonal in Fig. 12, whereas they need not be diagonal in Fig. 13. A full tuning capability is possible in Fig. 13, since $p = m(m+1) = 6$.

For a MAP AT which is reciprocal with respect to its radio ports and antenna ports, and for a duplex technique which utilizes the same frequencies for emission and reception, if we further assume that the antenna array is reciprocal and that the radio ports see a linear multiport generator of internal impedance matrix \mathbf{Z}_S during emission, and a linear and reciprocal multiport load of impedance matrix \mathbf{Z}_S during reception, we can assert that [81]-[82]:

- the set of the values of the transducer power gain during emission, obtained for all nonzero excitations, has a least element referred to as “minimum value”, and a greatest element referred to as “maximum value”;
- the set of the values of the transducer power gain during reception, obtained for all nonzero excitations, has a least element referred to as “minimum value”, and a greatest element referred to as “maximum value”;
- the maximum value of the transducer power gain during emission and the maximum value of the transducer power gain during reception are equal; and
- if $m = n$, the minimum value of the transducer power gain during emission and the minimum value of the transducer power gain during reception are equal.

It follows that, for a TDD transceiver using the same antennas and the same frequencies for emission and reception, an adjustment of the MAP AT which is good (or optimal) for emission, is also good (or optimal) for reception, if the stated assumptions hold.

C. SOME RELEVANT MAP AT CONTROL SCHEMES

The definition of type 0 control schemes in Section III can be used without modification with any MAP AT. Subtype *a* does not require any comment. For subtype *b*, it is advisable to use a plurality of localization variables, because antennas at different locations have different relative positions with nearby things or body parts [83].

We now look at the control schemes which use the configurations comprising SUs coupled either to the radio ports or to the antenna ports, to see if and how each type and subtype defined for SAP ATs can be adapted to MAP ATs.

If there is no significant coupling between the n antennas, for all relevant EECS, it is possible (and highly advisable) to use a MAP AT consisting of n uncoupled SAP ATs, each having a separate control system using a single SU according to one of the control schemes considered above in Section IV to Section IX. Preferably, such separate control systems could adjust the SAP ATs during tuning sequences which do not overlap in time, to avoid any interaction between the tuning sequences, through antenna coupling.

If a significant coupling exists or may exist between at least 2 of the $n \geq 2$ antennas, we may say that:

TABLE 2. Some possible characteristics of the MAP AT control scheme types and subtypes defined in Section XI.

Type	Figure	Subtype	Measurement	Mitigation of EECS	Aim of control	Accuracy	Speed
0	–	<i>a</i>	none	no	any	poor	very fast
		<i>b</i>	auxiliary variable	limited	any	poor	very fast
1	11(a)	<i>b</i>	vector at radio port	yes	$\mathbf{Z}_U = \mathbf{Z}_W$	very good	fast
		<i>c</i>	vector at radio port	yes	$\mathbf{Z}_U = \mathbf{Z}_W$	good / very good	very fast / fast
2	11(a)	<i>b</i>	vector at radio port	yes	$\mathbf{Z}_U = \mathbf{Z}_W$	very good	slow / very slow
3	11(b)	–	vector at antenna port	yes	any	good	very fast

- a MAP AT consisting of n uncoupled SAP ATs is usually not optimal, since it does not provide a full tuning capability, but it can nevertheless be selected, for instance based on cost or size considerations;
- it is incorrect to control each SAP AT of this MAP AT by utilizing a separate control system using a single SU, as if coupling through the antennas could be ignored.

In what follows, we consider control schemes that are compatible with coupling between the antennas. Such control schemes can be used with any type of MAP AT.

To obtain suitable information from the sensing unit output signals, the m TX ports of the TSPU deliver m excitations, one and only one of the excitations being delivered by each TX port, so that one and only one of the excitations is applied to each of the radio ports of the AT. It is possible that the m excitations are delivered successively by the TX ports [84]. A more general choice is to use excitations such that, with respect to the carrier frequency f_C , the m complex envelopes of the m excitations are linearly independent in the set of complex functions of one real variable, regarded as a vector space over the field of complex numbers [85]–[87].

Extracting suitable information from the sensing unit output signals, for such excitations, requires some computation, as explained in Appendix C. This precludes continuous-time control schemes. Thus, the type 1 subtype *a* and type 2 subtype *a* defined for SAP AT cannot be adapted to a MAP AT and will not be considered further.

In the following presentation of the possible types, we shall use the user port tuning range, denoted by $D_{UTR}(\mathbf{Z}_W)$, defined as the set of all \mathbf{Z}_{Sant} for which there exist achievable values of the nominal reactances of the AIDs, such that $\mathbf{Z}_U = \mathbf{Z}_W$ at f_C [10].

Type 1 designates the closed-loop control schemes which use SUs coupled to the radio ports, and are such that the TCSs are determined by a feedback control system which seeks to obtain a wanted value \mathbf{Z}_W of \mathbf{Z}_U at f_C , without implementing extremum-seeking control. Typically, the TSPU estimates q real quantities depending on \mathbf{Z}_U , where $q = 2m^2$. Since continuous-time control is ruled out, we can only identify 2 subtypes.

Type 1 subtype *b* designates the non-model-based schemes utilizing discrete-time control. We are not aware of any description of a type 1 subtype *b* control scheme. However,

the error of a type 1 subtype *b* control scheme is determined in subsection *B* of Appendix D.

Type 1 subtype *c* designates the model-based discrete-time control schemes [87]. More precisely, such a control scheme is based on a model of the AT and of the CU. For instance, let us assume that the AT is the one shown in Fig. 12 or the one shown in Fig. 13, that the nominal reactance of any one of the AIDs is determined by a tuning unit adjustment instruction received by the CU, and that \mathbf{Z}_U has been estimated, at f_C , for nominal AID reactances determined by an initial tuning unit adjustment instruction. In a first step, the TSPU estimates \mathbf{Y}_A , \mathbf{Z}_{AU} and \mathbf{Y}_U using the model and the initial tuning unit adjustment instruction, and then \mathbf{Z}_{Sant} using

$$\mathbf{Z}_{Sant} = (((\mathbf{Z}_U^{-1} - \mathbf{Y}_U)^{-1} - \mathbf{Z}_{AU})^{-1} - \mathbf{Y}_A)^{-1}. \quad (12)$$

If the estimated \mathbf{Z}_{Sant} lies in or close to the user port tuning range $D_{UTR}(\mathbf{Z}_W)$ of the AT at f_C , the TSPU can, in a second step, compute a subsequent tuning unit adjustment instruction such that, according to the model, \mathbf{Z}_U at f_C is close to \mathbf{Z}_W . This computation may for instance use the fast algorithm proposed in [27, Section 4], which takes losses in the AT into account. The operation of the control system may stop at this point, so that the nominal AID reactances directly jump from the ones determined by the initial tuning unit adjustment instruction, to the ones determined by the subsequent tuning unit adjustment instruction, by utilizing the model twice. The error of a type 1 subtype *c* control scheme, at the end of the adjustment sequence that we have just described, is determined in subsection *E* of Appendix D.

If the model of the AT and of the CU is not accurate, the subsequent tuning unit adjustment instruction may produce a \mathbf{Z}_U at f_C which is not close to \mathbf{Z}_W . In subsection *F* of Appendix D, it is shown that, in this case, repeating the steps that we have just described typically reduces the error of the type 1 subtype *c* control scheme, and makes the error almost independent of the accuracy of the model.

Type 2 designates the closed-loop control schemes which use SUs coupled to the radio ports, and in which the TSPU uses extremum-seeking control to obtain that \mathbf{Z}_U at f_C approximates a wanted value \mathbf{Z}_W [84], [85]. Continuous-time control being ruled out, only subtype *b*, which utilizes discrete-time extremum-seeking, exists. The performance variable may be any monotone function of a norm of the

image of \mathbf{Z}_U under a suitable matrix function, the matrix function being for instance one of the functions h mentioned in subsection A of Appendix D. In contrast to the SAP AT case, we are not aware of a simple manipulation providing a suitable performance variable from scalar measurements. Thus, unfortunately, we must assume that vector measurements at the radio ports are required for type 2 in the MAP AT case. Also, type 2 is slower for a MAP AT than for a SAP AT. In fact, the greater p , the slower the control scheme, because the extremum-seeking control algorithm must seek an extremum in a space of dimension p .

The error of a type 2 control scheme is computed in subsection B of Appendix D.

Type 3 designates the model-based control schemes which use SUs coupled to the antenna ports, and in which: the TSPU estimates q real quantities depending on \mathbf{Z}_{Sant} at f_C ; and the nominal reactance (or an equivalent variable) of at least one AID is determined as a function of f_C and of these real quantities, using a model of the AT and of the CU [86]. Typically, $q = 2n^2$. Type 3 is an open-loop control scheme which relies on an accurate model. Thus, if temperature is a relevant parameter, it should be measured and taken into account. The aim of a type 3 control scheme is unconstrained.

If the aim of the control scheme is to obtain a wanted value \mathbf{Z}_W of \mathbf{Z}_U at f_C , the type 3 control scheme is similar to the second step of the operation of a type 1 subtype c control scheme. In the case of an AT having the structure of a multidimensional π -network, suitable TCSs may be determined using the iterative computation technique of [27, Section 4], or a numerical algorithm that minimizes a suitable performance variable, for instance the square of a norm of $\mathbf{Z}_U - \mathbf{Z}_W$ computed using the model of the AT and of the CU.

The error of a type 3 control scheme is determined in subsection D of Appendix D.

Last and least, type 4 cannot be adapted to MAP ATs, because maximizing the average power delivered by the antenna ports is not a legitimate aim for wireless transmission using multiple antennas.

The applicable considerations of Section IX-A lead us to consider that any practical type 1 or type 2 control scheme for a MAP AT includes a preliminary open-loop step, of type 0. Thus, closed-loop control designs use lookup tables, because they are unavoidable for an open-loop control step.

Based on the foregoing, we have established Table 2, by utilizing an approach similar to the one used in Section IX.

D. OTHER MAP AT CONTROL SCHEMES

We have defined four types of control scheme which can be used to automatically adjust a MAP AT of a radio transmitter. Other control schemes are of course possible.

A MAP AT may be used in conjunction with TPAs [88]-[92]. As said for a SAP AT in Section VIII, this combination can provide a broader tuning range than the one provided by the AT alone, and reduced feeder losses. An automatic AT control system may use the adjustment of the TPAs to obtain a coarse adjustment of \mathbf{Z}_{Sant} , and then use the MAP AT to

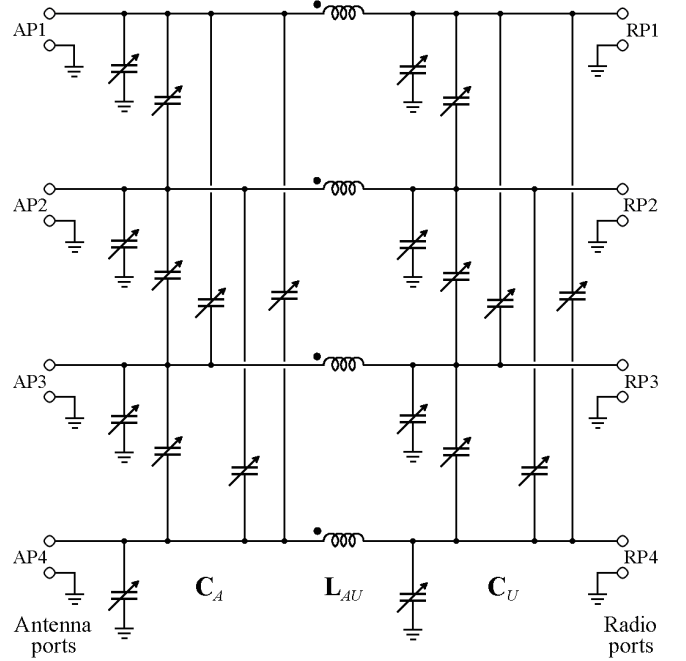


FIGURE 14. A MAP AT having 4 antenna ports (denoted by AP1 to AP4) and 4 radio ports (denoted by RP1 to RP4). This AT has the structure of a multidimensional π -network.

obtain a fine adjustment, using any type of control scheme. It is also possible to combine antenna selection, that is to say the selection of $n \geq 2$ antennas or TPAs among $N > n$ antennas or TPAs, with a MAP AT using any one of the control schemes [93].

An automatic MAP AT control system using a type 1, type 2 or type 3 control scheme may also, if this is relevant, seek and obtain an authorization from a wireless network, prior to let the TSPU deliver the excitations needed to perform the adjustment of the AT [94]-[96].

XII. EXAMPLE USING A MAP AT

Let q be a nonzero integer, $\mathbf{1}_q$ be the identity matrix of size q by q , and r_0 be an arbitrary resistance. For an arbitrary impedance matrix \mathbf{Z} of size q and the reference resistance r_0 , the return figure $F(\mathbf{Z})$ is the nonnegative real number defined by [10]:

$$F(\mathbf{Z}) = \|\mathbf{S}(\mathbf{Z})\|_2, \quad (13)$$

where $\mathbf{S}(\mathbf{Z})$ is a scattering matrix defined by

$$\begin{aligned} \mathbf{S}(\mathbf{Z}) &= (\mathbf{Z} + r_0 \mathbf{1}_q)^{-1} (\mathbf{Z} - r_0 \mathbf{1}_q) \\ &= (\mathbf{Z} - r_0 \mathbf{1}_q) (\mathbf{Z} + r_0 \mathbf{1}_q)^{-1}, \end{aligned} \quad (14)$$

and where the spectral norm $\|\mathbf{A}\|_2$ of a square matrix \mathbf{A} is the largest singular value of \mathbf{A} [97, Section 5.6.6]. $F(\mathbf{Z})$ expressed in decibels is $F_{dB}(\mathbf{Z}) = 20 \log(F(\mathbf{Z}))$. It is the largest value of the ratio, expressed in decibels, of the reflected power to the incident power, for all possible nonzero excitations. In what follows, “decoupling and matching” means $\mathbf{Z}_U = \mathbf{Z}_W$, where $\mathbf{Z}_W = r_0 \mathbf{1}_m$, and $r_0 = 50 \Omega$. Decoupling and matching is exactly obtained if and only if $F(\mathbf{Z}_U) = 0$ or $F_{dB}(\mathbf{Z}_U) = -\infty$ dB.

The MAP AT shown in Fig. 14 has the structure of a multidimensional π -network. It comprises $p = m(m + 1) = 20$ AIDs presenting a negative reactance, depicted using the variable capacitor symbols in Fig. 14. Examples showed that it may have a full tuning capability, and that it can be adjusted to provide decoupling and matching over broad frequency ranges, and in the presence of EECS [10], [27], [68], [79].

It has also been shown, with a theoretical example, that $F(\mathbf{Z}_U)$ is not very sensitive to the values of the 20 AIDs [27]. This point is important for a preliminary open-loop step of a closed-loop control scheme (type 1 or type 2), and essential for the open-loop control schemes (type 0 or type 3). It is therefore interesting to summarize the results obtained about the sensitivity of the MAP AT of Fig. 14 to AID values, which are based on the following assumptions:

- the antennas are $n = 4$ side-by-side parallel lossless dipole antennas, each having a total length of 224.8 mm, the radius of the array being 56.2 mm, each antenna having a 60 mm long lossy feeder; and
- the components of the MAP AT have loss characteristics defined by a model similar to the one used in Section X, with $L_N = 2.7$ nH, $R_S \simeq 119$ m Ω , $R_P \simeq 20.7$ k Ω , $C \simeq 48.8$ fF, $\omega_P = 9 \times 10^6$ rd/s and $\omega_S = 3 \times 10^{12}$ rd/s.

In [27, Sec. 5], it is shown that an adjustment providing decoupling and matching exists at any tuning frequency in the frequency range 700 MHz to 900 MHz, and the corresponding capacitance values of the adjustable impedance devices are computed.

To obtain an accurate picture of the effect of simultaneous deviations of the capacitance of the 20 AIDs, we can assume independent normally distributed capacitance deviations, with a zero mean deviation from the computed values, and a specified relative standard deviation σ_C . At the tuning frequency of 800 MHz, we can determine the statistic of the return figure $F(\mathbf{Z}_U)$ in dB, the mean of $F(\mathbf{Z}_U)$ in dB, denoted by m_F , and the corrected sample standard deviation of $F(\mathbf{Z}_U)$ in dB, denoted by σ_F . The histogram of Fig. 15 shows the relative frequency of $F(\mathbf{Z}_U)$ in dB, obtained for $\sigma_C = 1\%$, with 10000 samples (of the MAP AT). The assumption $\sigma_C = 1\%$ could for instance correspond to a $\pm 3\%$ tolerance defined by a 3-sigma deviation. For the statistics shown in Fig. 15, we have $m_F \approx -27.22$ dB and $\sigma_F \approx 2.79$ dB. The maximum value of $F(\mathbf{Z}_U)$ is -19.00 dB, whereas, for a normal distribution the probability of having $F(\mathbf{Z}_U)$ greater than $m_F + 3\sigma_F \approx -18.86$ dB would be about 1.35×10^{-3} , corresponding to an expectation of about 13.5 for 10000 samples.

This data shows that a specified maximum return figure of $m_F + 3\sigma_F \approx -18.86$ dB, at the tuning frequency, can reliably be obtained with $\sigma_C = 1\%$. The specified maximum return figures of $m_F + 3\sigma_F$, at the tuning frequency, which can reliably be obtained with a given value of σ_C , may be derived from Fig. 16, which shows m_F and σ_F , as a function of σ_C , obtained with 1000 samples for each value of σ_C .

Thus, in this example, accurate preliminary open-loop steps and accurate open-loop control schemes are realisable, since the sensitivity of $F(\mathbf{Z}_U)$ to AID values is reasonable.

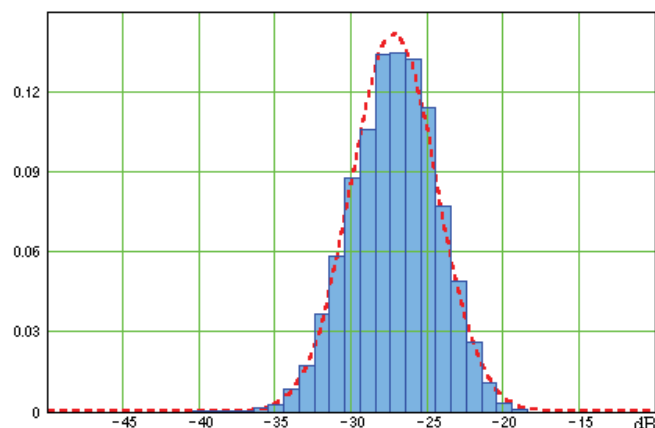


FIGURE 15. Histogram of the relative frequency of $F(\mathbf{Z}_U)$ in dB, for $\sigma_C = 1\%$, obtained with 10000 samples, and normal distribution having the same mean and the same standard deviation (dashed curve).

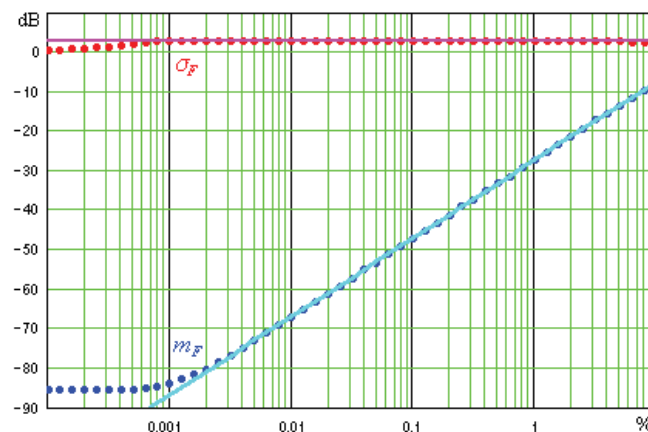


FIGURE 16. m_F and σ_F versus σ_C , and linear regression lines based on the values obtained for $0.01\% \leq \sigma_C \leq 10\%$.

XIII. CONCLUSION

An appropriate AT with a suitable control scheme can be used to obtain the best possible performance from one or more antennas or TPAs, over the broadest frequency range, and to adaptively compensate the EECS. It may also compensate some other causes of antenna performance degradation, such as manufacturing tolerances, aging, temperature, etc. Thus, it may be used to reduce antenna size and to simplify antenna or TPA design. In the case of MIMO transmission, an appropriate MAP AT with a suitable control scheme can also adaptively compensate the antenna interaction, that is, provide decoupling and matching. In this case, the acceptable coupling between antennas is increased, so that their separation could be reduced.

Five types of control scheme applicable to a SAP AT have been presented. Four of them are also applicable to a MAP AT. They have been compared as regards: their use of closed-loop control and/or open-loop control; the measurements used; their ability to mitigate the EECS; the aim of the control scheme; their accuracy and speed; and their dependence on a model of the AT and CU. Some aspects of the comparison are summarized in Table 1 and Table 2. This material should

help system designers to select the most appropriate control schemes for their applications.

Type 3 is an accurate and very fast open-loop scheme for which it might be useful to take into account one or more temperatures in the AT to determine the TCSs.

Type 4 control schemes are only applicable to SAP ATs, for which they provide the best transmitter efficiency, because they are accurate and their aim is maximizing P_{Sant} . They leave a residual VSWR, which should be small enough. Type 4 subtype a is inexpensive (because it uses scalar measurement), but not fast. Type 4 subtype b is more expensive, but it is faster.

For SAP ATs, the fastest schemes providing a good accuracy are type 1 subtype c , type 3, and type 4 subtype b , all of which use vector measurements. Type 1 subtype c combines high speed and accuracy. In contrast to type 3 and type 4 subtype b , it uses vector impedance measurements at the radio port. For this reason, it might be the best choice in most fast and accurate SAP designs.

If several antennas are used simultaneously and coupling between all antennas cannot be ignored, multiple independent SAP AT control schemes are not appropriate, even if the MAP AT is made of uncoupled SAP ATs.

For MAP ATs, the fastest schemes providing a good accuracy are type 1 subtype c and type 3, which both use vector measurements. Type 1 subtype c combines high speed and accuracy. In contrast to type 3, it uses vector impedance measurements at the radio ports. For this reason, it might be the best choice in most fast and accurate MAP designs.

Being not essential to define our typology of AT control schemes, the following subject matters have not been treated in this article: the design of SAP ATs, the design of MAP ATs, the design of SUs and the processing of sensing unit output signals. They are of course essential for the design of an optimal automatic antenna tuning system.

APPENDIX A

A. PURPOSE OF THIS APPENDIX AND NOTATIONS

In this Appendix A, we want to further explain and investigate different types of SAP AT control scheme which seek to obtain that Z_U at f_C is very close, or as close as possible, to a wanted impedance Z_W .

We need to clarify the meaning of “very close, or as close as possible, to a wanted impedance Z_W ”. Let us choose a complex function of a complex variable, denoted by h , the function being continuous and smooth where it is defined, and such that $h(Z_W) = 0$. For instance, the function may be defined by

$$h(Z) = Z - Z_W, \quad (15)$$

or by

$$h(Z) = Z^{-1} - Z_W^{-1}, \quad (16)$$

or by

$$h(Z) = (Z - Z_W)(Z + Z_W)^{-1}. \quad (17)$$

We say that Z is (very) close to Z_W if and only if $h(Z)$ is (very) close to zero; we say that Z is as close as possible to Z_W if and only if $h(Z)$ is as close as possible to zero; etc.

We assume a digital control system in which the nominal reactances (or equivalent variables) of the AIDs are, at a given point in time, determined by the CU as a function of a tuning unit adjustment instruction delivered by the TSPU. An exact numerical model of the AT and of the CU may be put in the form of a mapping denoted by g_{EU} and defined by

$$g_{EU}(f, Z_{Sant}, t_C, \mathbf{a}_T) = Z_U, \quad (18)$$

where f is the frequency, where t_C is the applicable tuning unit adjustment instruction, and where \mathbf{a}_T is a real vector of temperatures, which is sufficient to characterize the effects of temperature on Z_U . As an example, if the impedance of each AID depends on its temperature and if the characteristics of the CU do not significantly depend on temperature, the elements of \mathbf{a}_T could be the temperatures of the AIDs.

At the frequency f and for the temperatures specified in \mathbf{a}_T , the user port impedance range of the AT is given by

$$D_{UR}(Z_{Sant}) = \{g_{EU}(f, Z_{Sant}, t_C, \mathbf{a}_T) | t_C \in T_C\}, \quad (19)$$

where T_C is the set of the possible tuning unit adjustment instructions [10].

B. NON-MODEL-BASED DIGITAL CLOSED-LOOP SAP AT CONTROL SCHEMES

In a non-model-based digital closed-loop control scheme (that is, a type 1 subtype b or type 2 subtype b scheme), a full automatic adjustment of the AT requires several iterations, each iteration comprising the following steps: applying an excitation to the radio port; sensing electrical variables at the radio port; delivering a tuning unit adjustment instruction; and delivering TCSs. After a sufficient number of iterations, a final tuning unit adjustment instruction t_{CF} is reached. If the control scheme is well-designed, the measured value of Z_U at f_C while t_{CF} is applicable, denoted by Z_{UM} , satisfies

$$Z_{UM} \simeq Z_W - d_{QCL1}(f_C, Z_{Sant}, t_C, \mathbf{a}_T), \quad (20)$$

where the mapping d_{QCL1} represents a quantization error which is known to the control system, but which cannot be avoided because there is no t_C in T_C such that Z_{UM} is closer to Z_W . Thus, the error of the control system is given by

$$Z_U - Z_W \simeq Z_U - Z_{UM} - d_{QCL1}(f_C, Z_{Sant}, t_C, \mathbf{a}_T), \quad (21)$$

where $Z_U - Z_{UM}$ is the measurement error.

C. ADDITIONAL ASSUMPTIONS FOR MODEL-BASED SAP AT CONTROL SCHEMES

In a model-based digital control scheme (that is, a type 1 subtype c or type 3 scheme), we assume that the TSPU, instead of knowing the exact numerical model of the AT and of the CU, corresponding to g_{EU} , knows an approximate

numerical model of the AT and of the CU, which corresponds to a mapping g_{AU} such that

$$g_{AU}(f, Z_{Sant}, t_C, \mathbf{a}_T) + d_{AU}(f, Z_{Sant}, t_C, \mathbf{a}_T) = Z_U, \quad (22)$$

where the mapping d_{AU} represents the error of the approximate numerical model, and is not known to the control system.

D. TYPE 3 SAP AT CONTROL SCHEME

A type 3 control scheme uses a measurement Z_{SantM} of Z_{Sant} at f_C , and possibly a measurement \mathbf{a}_{TM} of \mathbf{a}_T . Here, a suitable algorithm is used to find a tuning unit adjustment instruction, denoted by t_{CS} , such that $g_{AU}(f_C, Z_{SantM}, t_{CS}, \mathbf{a}_{TM})$ is very close, or as close as possible, to the wanted impedance Z_W . We write

$$g_{AU}(f_C, Z_{SantM}, t_{CS}, \mathbf{a}_{TM}) + d_{QOL}(f_C, Z_{SantM}, t_{CS}, \mathbf{a}_{TM}) = Z_W, \quad (23)$$

where the mapping d_{QOL} represents a quantization error which is known to the control system, but which cannot be avoided because there is no t_C in T_C such that $g_{AU}(f_C, Z_{SantM}, t_C, \mathbf{a}_{TM})$ is closer to Z_W . The resulting Z_U at f_C is given by

$$g_{AU}(f_C, Z_{Sant}, t_{CS}, \mathbf{a}_T) + d_{AU}(f_C, Z_{Sant}, t_{CS}, \mathbf{a}_T) = Z_U. \quad (24)$$

Thus, the error of the control system is given by

$$Z_U - Z_W = g_{AU}(f_C, Z_{Sant}, t_{CS}, \mathbf{a}_T) - g_{AU}(f_C, Z_{SantM}, t_{CS}, \mathbf{a}_{TM}) + d_{AU}(f_C, Z_{Sant}, t_{CS}, \mathbf{a}_T) - d_{QOL}(f_C, Z_{SantM}, t_{CS}, \mathbf{a}_{TM}), \quad (25)$$

in which the first 2 terms of the right-hand side vanish for exact measurements.

E. TYPE 1 SUBTYPE C SAP AT CONTROL SCHEME

In a type 1 subtype c control scheme, an adjustment sequence comprises the following steps: an initial tuning unit adjustment instruction t_{CI} is delivered by the TSPU; a measurement Z_{UIM} of Z_{UI} is obtained, where Z_{UI} is the value of Z_U at f_C while t_{CI} is applicable; and a subsequent tuning unit adjustment instruction t_{CS} is computed as explained below, and delivered by the TSPU [23]–[24]. While t_{CI} is applicable, we have

$$g_{AU}(f_C, Z_{Sant}, t_{CI}, \mathbf{a}_T) + d_{AU}(f_C, Z_{Sant}, t_{CI}, \mathbf{a}_T) = Z_{UI}. \quad (26)$$

Let \mathbf{a}_{TM} be an estimate of \mathbf{a}_T , possibly based on a measurement. The TSPU solves the equation

$$g_{AU}(f_C, Z_{SantE}, t_{CI}, \mathbf{a}_{TM}) = Z_{UIM} \quad (27)$$

with respect to the unknown Z_{SantE} , to obtain an estimated value Z_{SantE} of Z_{Sant} . Thus, we have

$$Z_{UI} - Z_{UIM} = g_{AU}(f_C, Z_{Sant}, t_{CI}, \mathbf{a}_T) - g_{AU}(f_C, Z_{SantE}, t_{CI}, \mathbf{a}_{TM}) + d_{AU}(f_C, Z_{Sant}, t_{CI}, \mathbf{a}_T). \quad (28)$$

Z_{SantE} and \mathbf{a}_{TM} are then used by a suitable algorithm to determine t_{CS} such that $g_{AU}(f_C, Z_{SantE}, t_{CS}, \mathbf{a}_{TM})$ is very close, or as close as possible, to the wanted impedance Z_W . We note that this step is similar to the one leading to (23). We may write

$$g_{AU}(f_C, Z_{SantE}, t_{CS}, \mathbf{a}_{TM}) + d_{QCL2}(f_C, Z_{SantE}, t_{CS}, \mathbf{a}_{TM}) = Z_W, \quad (29)$$

where the mapping d_{QCL2} represents a quantization error which is known to the control system, but which cannot be avoided because there is no t_C in T_C such that $g_{AU}(f_C, Z_{SantE}, t_C, \mathbf{a}_{TM})$ is closer to Z_W . The resulting Z_U at f_C while t_{CS} is applicable is given by

$$g_{AU}(f_C, Z_{Sant}, t_{CS}, \mathbf{a}_T) + d_{AU}(f_C, Z_{Sant}, t_{CS}, \mathbf{a}_T) = Z_U. \quad (30)$$

Thus, the error of the control system while t_{CS} is applicable is given by

$$Z_U - Z_W = g_{AU}(f_C, Z_{Sant}, t_{CS}, \mathbf{a}_T) - g_{AU}(f_C, Z_{SantE}, t_{CS}, \mathbf{a}_{TM}) + d_{AU}(f_C, Z_{Sant}, t_{CS}, \mathbf{a}_T) - d_{QCL2}(f_C, Z_{SantE}, t_{CS}, \mathbf{a}_{TM}), \quad (31)$$

in which the first 3 terms of the right-hand side vanish for exact measurements and an exact numerical model. Let us use Λ_{AU} to denote the mapping such that

$$\begin{aligned} \Lambda_{AU}(f_C, Z_{Sant}, Z_{SantE}, t_{CS}, t_{CI}, \mathbf{a}_T, \mathbf{a}_{TM}) &= \\ &= g_{AU}(f_C, Z_{Sant}, t_{CS}, \mathbf{a}_T) - g_{AU}(f_C, Z_{SantE}, t_{CS}, \mathbf{a}_{TM}) \\ &\quad + d_{AU}(f_C, Z_{Sant}, t_{CS}, \mathbf{a}_T) \\ &\quad - [g_{AU}(f_C, Z_{Sant}, t_{CI}, \mathbf{a}_T) - g_{AU}(f_C, Z_{SantE}, t_{CI}, \mathbf{a}_{TM}) \\ &\quad \quad + d_{AU}(f_C, Z_{Sant}, t_{CI}, \mathbf{a}_T)]. \quad (32) \end{aligned}$$

For any values of f_C , Z_{Sant} , Z_{SantE} , t_{CI} , \mathbf{a}_T and \mathbf{a}_{TM} , we have

$$\Lambda_{AU}(f_C, Z_{Sant}, Z_{SantE}, t_{CI}, t_{CI}, \mathbf{a}_T, \mathbf{a}_{TM}) = 0. \quad (33)$$

It follows from (28) and (32) that

$$\begin{aligned} Z_{UI} - Z_{UIM} &+ \Lambda_{AU}(f_C, Z_{Sant}, Z_{SantE}, t_{CS}, t_{CI}, \mathbf{a}_T, \mathbf{a}_{TM}) = \\ &= g_{AU}(f_C, Z_{Sant}, t_{CS}, \mathbf{a}_T) - g_{AU}(f_C, Z_{SantE}, t_{CS}, \mathbf{a}_{TM}) \\ &\quad + d_{AU}(f_C, Z_{Sant}, t_{CS}, \mathbf{a}_T). \quad (34) \end{aligned}$$

Substituting (34) in (31), we can write that the error of the control system while t_{CS} is applicable is given by

$$Z_U - Z_W = Z_{UI} - Z_{UIM} + \Lambda_{AU}(f_C, Z_{Sant}, Z_{SantE}, t_{CS}, t_{CI}, \mathbf{a}_T, \mathbf{a}_{TM}) - d_{QCL2}(f_C, Z_{SantE}, t_{CS}, \mathbf{a}_{TM}). \quad (35)$$

By (27), Z_{SantE} may be regarded as a function of f_C , t_{CI} , \mathbf{a}_{TM} and Z_{UIM} . Thus, by (29), t_{CS} may be regarded as a function of f_C , t_{CI} , \mathbf{a}_{TM} , Z_{UIM} and Z_W . Thus, by (32), $\Lambda_{AU}(f_C, Z_{Sant}, Z_{SantE}, t_{CS}, t_{CI}, \mathbf{a}_T, \mathbf{a}_{TM})$ may be regarded as a function of f_C , Z_{Sant} , t_{CI} , \mathbf{a}_T , \mathbf{a}_{TM} , Z_{UIM} and Z_W . Thus, we can define the mapping E_{AU} such that

$$E_{AU}(f_C, Z_{Sant}, t_{CI}, \mathbf{a}_T, \mathbf{a}_{TM}, Z_{UIM}, Z_W) = \Lambda_{AU}(f_C, Z_{Sant}, Z_{SantE}, t_{CS}, t_{CI}, \mathbf{a}_T, \mathbf{a}_{TM}). \quad (36)$$

If $Z_{UIM} = Z_W$, the control system believes that it has reached Z_W , so that $t_{CS} = t_{CI}$. Thus, using (33) and (36), we obtain that for any values of f_C , Z_{Sant} , t_{CI} , \mathbf{a}_T , \mathbf{a}_{TM} and Z_W , we have

$$E_{AU}(f_C, Z_{Sant}, t_{CI}, \mathbf{a}_T, \mathbf{a}_{TM}, Z_W, Z_W) = 0. \quad (37)$$

With respect to the variable Z_{UIM} of (36), the mapping E_{AU} is probably neither smooth nor continuous, because of the quantization error and possibly other reasons. However, let us assume that the control system and its numerical model are such that, with respect to the variable Z_{UIM} , the mapping E_{AU} may be approximately considered as continuous. Thus, by (37), if Z_{UIM} is sufficiently close to Z_W , then $E_{AU}(f_C, Z_{Sant}, t_{CI}, \mathbf{a}_T, \mathbf{a}_{TM}, Z_{UIM}, Z_W)$ is close to 0 and $\Lambda_{AU}(f_C, Z_{Sant}, Z_{SantE}, t_{CS}, t_{CI}, \mathbf{a}_T, \mathbf{a}_{TM})$ is close to 0. Thus, if Z_{UIM} is sufficiently close to Z_W , the error of the control system while t_{CS} is applicable satisfies

$$Z_U - Z_W \simeq Z_{UI} - Z_{UIM} - d_{QCL2}(f_C, Z_{SantE}, t_{CS}, \mathbf{a}_{TM}). \quad (38)$$

According to (38), the error of the control system while t_{CS} is applicable is almost equal to the measurement error $Z_{UI} - Z_{UIM}$ less the quantization error. If we compare (38) to (35), we observe that a cancellation of errors has occurred. Also, the error given by (38) is to a large extent independent of the accuracy of the approximate numerical model, and (38) is similar to (21) established for a non-model-based closed-loop control system. This advantage is a consequence of the fact that the control system has used the approximate numerical model of the AT and of the CU twice: the first time to estimate Z_{SantE} , and the second time to determine t_{CS} .

F. TYPE 1 SUBTYPE C WITH ITERATION FOR A SAP AT

Let us now assume that the adjustment sequence considered so far has used an initial tuning unit adjustment instruction t_{CI} such that Z_{UIM} need not be sufficiently close to Z_W to obtain that the error of the control system at the end of this first adjustment sequence satisfies (38). Thus, at the end of this first adjustment sequence, the error is given by (35). We can now introduce an iteration, in which the

first adjustment sequence is quickly followed by a second adjustment sequence, such that the subsequent tuning unit adjustment instruction of the first adjustment sequence becomes the initial tuning unit adjustment instruction of a second adjustment sequence. If the first adjustment sequence is sufficiently accurate, the second adjustment sequence uses an initial tuning unit adjustment instruction such that Z_{UIM} is sufficiently close to Z_W to obtain that the error of the control system at the end of the second adjustment sequence satisfies (38). Thus, under this assumption, thanks to the iteration, a cancellation of errors is obtained, such that the error of the control system at the end of the second adjustment sequence becomes to a large extent independent of the accuracy of the approximate numerical model.

APPENDIX B

In this Appendix B, we want to further explain and investigate different types of SAP AT control scheme which seek to maximize P_{Sant} at f_C .

We assume a digital control system in which the nominal reactances (or equivalent variables) of the AIDs are, at a given point in time, determined by the CU as a function of a tuning unit adjustment instruction delivered by the TSPU. An exact numerical model of the AT, of the CU, and of the TX port of the TSPU while the TSPU delivers the excitation (this port need not be linear), may be put in the form of a mapping denoted by p_E and defined by

$$p_E(f, Z_{Sant}, t_C, \mathbf{a}_T) = P_{Sant}, \quad (39)$$

where f is the frequency, where t_C is the applicable tuning unit adjustment instruction, and where \mathbf{a}_T is a real vector of temperatures, which is sufficient to characterize the effects of temperature on P_{Sant} .

In a type 4 subtype *a* or type 4 subtype *b* control scheme, a full automatic adjustment of the AT requires several non-model-based iterations, each iteration comprising the following steps: applying an excitation to the radio port; sensing one or more electrical variables at the antenna port; estimating the performance variable; delivering a tuning unit adjustment instruction; and delivering TCSs. After a sufficient number of iterations, a final tuning unit adjustment instruction t_{CF} is reached. If the control scheme is well-designed, t_{CF} maximizes P_{Sant} at f_C . Thus, t_{CF} satisfies

$$t_{CF} = \operatorname{argmax}_{t_C \in T_C} p_E(f_C, Z_{Sant}, t_C, \mathbf{a}_T), \quad (40)$$

where T_C is the set of the possible tuning unit adjustment instructions. Here, the control system reaches its aim, exactly, and there is no effect of measurement errors, under the assumption that the performance variable is a monotone function of P_{Sant} .

In a type 3 control scheme, which is model-based, we assume that the TSPU, instead of knowing the exact numerical model of the AT, of the CU, and of the TX port of the TSPU, corresponding to p_E , knows an approximate

numerical model of the AT, of the CU, and of the TX port of the TSPU, which corresponds to a mapping p_A such that

$$p_A(f, Z_{Sant}, t_C, \mathbf{a}_T) + q_A(f, Z_{Sant}, t_C, \mathbf{a}_T) = P_{Sant}, \quad (41)$$

where the mapping q_A represents the error of the approximate numerical model, and is not known to the control system.

The type 3 control scheme uses a measurement Z_{SantM} of Z_{Sant} at f_C , and possibly a measurement \mathbf{a}_{TM} of \mathbf{a}_T . Here, a suitable algorithm is used to find a tuning unit adjustment instruction, denoted by t_{CS} , such that $p_A(f_C, Z_{SantM}, t_{CS}, \mathbf{a}_{TM})$ is as large as possible. Thus, t_{CS} satisfies

$$t_{CS} = \operatorname{argmax}_{t_C \in T_C} p_A(f_C, Z_{SantM}, t_C, \mathbf{a}_{TM}), \quad (42)$$

and the error of the control system is given by

$$\Delta P_{Sant} = p_E(f_C, Z_{Sant}, t_{CS}, \mathbf{a}_T) - \max_{t_C \in T_C} p_E(f_C, Z_{Sant}, t_C, \mathbf{a}_T). \quad (43)$$

This error depends on the accuracy of the model. It vanishes for exact measurements and an exact model.

APPENDIX C

A. PURPOSE AND ASSUMPTIONS

In this Appendix C, we provide theoretical examples that clarify how, in a MAP AT control scheme, the sensing unit output signals may be processed to fully determine \mathbf{Z}_U at f_C in the configuration where the SUs are coupled to the m radio ports, shown in Fig. 11(a) for $m = n = 2$; or to fully determine \mathbf{Z}_{Sant} at f_C in the configuration where the SUs are coupled to n antenna ports, shown in Fig. 11(b) for $m = n = 2$.

Let us number the radio ports from 1 to m , and let us number the excitations from 1 to m , in such a way that, if we use t to denote time, for any $a \in \{1, \dots, m\}$, the excitation number a consists of an open-circuit voltage $v_{OCa}(t)$ applied to the radio port number a . We assume that $v_{OCa}(t)$ is a bandpass signal of carrier frequency f_C and of complex envelope $v_{EOCa}(t)$. Let E be any suitable subspace of the set of complex functions of one real variable, regarded as a vector space over the field of complex numbers. We assume that the complex envelopes $v_{EOC1}(t), \dots, v_{EOCm}(t)$ are linearly independent in E . To obtain this result, we may for instance use m excitations that are delivered successively by the TX ports, or orthogonal excitations, or excitations obtained as explained below at the end of subsection E. We assume that, while the excitations are delivered by the TSPU, the radio ports see a linear multiport source of impedance matrix \mathbf{Z}_L , which has a positive definite hermitian part, so that it is the impedance matrix of a strictly passive network. Note that, if \mathbf{Z}_L is created by the outputs of uncoupled power amplifiers, \mathbf{Z}_L is diagonal, but we do not need this assumption.

B. PSEUDO-COORDINATES

Let W be a bandwidth of the excitations. Since, for any $a \in \{1, \dots, m\}$, the real signal $v_{OCa}(t)$ is a bandpass signal of carrier frequency f_C and of complex envelope $v_{EOCa}(t)$, it follows that $v_{OCa}(t)$ has a Fourier transform, denoted by $V_{OCa}(f)$, and that $v_{EOCa}(t)$ has a Fourier transform, denoted by $V_{EOCa}(f)$ and such that [98, Sec. 2.2.2]-[99, Sec. 2.1-2]

$$f \notin [-W/2, W/2] \Rightarrow V_{EOCa}(f) = 0, \quad (44)$$

and

$$f \in [-\frac{W}{2}, \frac{W}{2}] \Rightarrow V_{EOCa}(f) = kV_{OCa}(f + f_C), \quad (45)$$

where k is a dimensionless real constant which is chosen equal to $\sqrt{2}$ by some authors.

Let $x(t)$ be any voltage or current measured at anyone of the antenna ports or radio ports. We assume that the effects on the antennas, of electromagnetic fields caused by external sources, can be ignored. The AT being linear with respect to its antenna ports and radio ports, $x(t)$ has a Fourier transform, denoted by $X(f)$, which at any frequency f satisfies

$$X(f) = \sum_{a=1}^m \lambda_a(f) V_{OCa}(f), \quad (46)$$

where, for any $a \in \{1, \dots, m\}$, $\lambda_a(f)$ is a dimensionless complex function if $x(t)$ is a voltage, or a complex function having the dimensions of admittance if $x(t)$ is a current. Thus, $x(t)$ is a bandpass signal of carrier frequency f_C , of complex envelope $x_E(t)$, the Fourier transform of $x_E(t)$, denoted by $X_E(f)$ being such that

$$f \notin [-W/2, W/2] \Rightarrow X_E(f) = 0, \quad (47)$$

and

$$f \in [-W/2, W/2] \Rightarrow X_E(f) = k \sum_{a=1}^m \lambda_a(f + f_C) V_{OCa}(f + f_C). \quad (48)$$

Using (44) and (45) in (47) and (48), respectively, we obtain

$$X_E(f) = \sum_{a=1}^m \lambda_a(f + f_C) V_{EOCa}(f). \quad (49)$$

If W is sufficiently small compared to f_C , then $\lambda_a(f + f_C)$ is almost constant over $[-W/2, W/2]$, so that

$$X_E(f) \simeq \sum_{a=1}^m \lambda_a(f_C) V_{EOCa}(f), \quad (50)$$

and

$$x_E(t) \simeq \sum_{a=1}^m \lambda_a(f_C) v_{EOCa}(t). \quad (51)$$

Let S be the span of $v_{EOC1}(t), \dots, v_{EOCm}(t)$ in E . Since $v_{EOC1}(t), \dots, v_{EOCm}(t)$ are assumed to be linearly independent, they form a basis \mathcal{B} of S . In what follows, based

on (51), $\lambda_1(f_C), \dots, \lambda_m(f_C)$ are referred to as the “pseudo-coordinates” of $x_E(t)$ in \mathcal{B} . These pseudo-coordinates are complex and time-independent.

By (46), $x(t)$ is exactly a sum of m components, each being the part of $x(t)$ caused by one of the excitations, and each being a bandpass signal of carrier frequency f_C . By (49), $x_E(t)$ is exactly a sum of m components, each being the part of $x_E(t)$ caused by one of the excitations, and each being the complex envelope of the part of $x(t)$ caused by this excitation. Thus, if W is sufficiently narrow, it follows from (51) that, for any $a \in \{1, \dots, m\}$, the complex envelope of the part of $x(t)$ caused by excitation a , which is equal to the part of $x_E(t)$ caused by excitation a , is approximately $\lambda_a(f_C)v_{EOC_a}(t)$. We have consequently shown that, if W is sufficiently narrow, then for any $a \in \{1, \dots, m\}$, the part caused by excitation a , of a voltage or current $x(t)$ measured at anyone of the antenna ports or radio ports, is a bandpass signal of carrier frequency f_C , the complex envelope of this bandpass signal being nearly $v_{EOC_a}(t)$ times the a -th pseudo-coordinate of the complex envelope of $x(t)$ in \mathcal{B} .

C. SENSING UNITS AT THE RADIO PORTS

We now outline an example of signal processing for the configuration in which the sensing unit output signals are determined by electrical variables sensed at the m radio ports. For simplicity, we may for instance assume that the electrical variables are the voltages and currents at the radio ports.

For any $b \in \{1, \dots, m\}$, we can use $i_{Rb}(t)$ to denote the current flowing into radio port b , and $v_{Rb}(t)$ to denote the voltage across radio port b . As explained above, $i_{Rb}(t)$ and $v_{Rb}(t)$ are bandpass signals of carrier frequency f_C . Let $i_{ERb}(t)$ and $v_{ERb}(t)$ be the complex envelopes of $i_{Rb}(t)$ and $v_{Rb}(t)$, respectively, for this carrier frequency.

For any $a \in \{1, \dots, m\}$, we can use \mathbf{u}_{ERa} to denote the column vector of the a -th pseudo-coordinates of the complex envelopes $v_{ER1}(t), \dots, v_{ERm}(t)$ in \mathcal{B} , and \mathbf{j}_{ERa} to denote the column vector of the a -th pseudo-coordinates of the complex envelopes $i_{ER1}(t), \dots, i_{ERm}(t)$ in \mathcal{B} . If the bandwidth of the complex envelopes $v_{EOC_1}(t), \dots, v_{EOC_m}(t)$ is sufficiently narrow, by (46) and (51), for any $a \in \{1, \dots, m\}$, we have

$$\mathbf{j}_{ERa} \simeq (\mathbf{Z}_U + \mathbf{Z}_L)^{-1} \mathbf{E}_a, \quad (52)$$

where \mathbf{E}_a is a complex vector of size m , the entries of which are zero except the entry of row a which is equal to 1, and

$$\mathbf{u}_{ERa} \simeq \mathbf{Z}_U \mathbf{j}_{ERa}. \quad (53)$$

In (52) and (53), \mathbf{Z}_U and \mathbf{Z}_L are considered at f_C .

Let \mathbf{U}_{ER} be the complex matrix of size m by m whose column vectors are $\mathbf{u}_{ER1}, \dots, \mathbf{u}_{ERm}$, and \mathbf{J}_{ER} be the complex matrix of size m by m whose column vectors are $\mathbf{j}_{ER1}, \dots, \mathbf{j}_{ERm}$. \mathbf{U}_{ER} is dimensionless, and \mathbf{J}_{ER} has the dimensions of admittance. By (52) we have

$$\mathbf{J}_{ER} \simeq (\mathbf{Z}_U + \mathbf{Z}_L)^{-1}. \quad (54)$$

$\mathbf{Z}_U + \mathbf{Z}_L$ being the impedance matrix of a strictly passive network, its hermitian part is positive definite, so that it is

invertible [81, Lemma 1]. Thus, \mathbf{J}_{ER} is correctly determined by (54). By (53), we have

$$\mathbf{U}_{ER} \simeq \mathbf{Z}_U \mathbf{J}_{ER}. \quad (55)$$

It follows from (54) that \mathbf{J}_{ER} is invertible, so that

$$\mathbf{Z}_U \simeq \mathbf{U}_{ER} \mathbf{J}_{ER}^{-1}. \quad (56)$$

The entries of \mathbf{U}_{ER} are pseudo-coordinates of the complex envelopes $v_{ER1}(t), \dots, v_{ERm}(t)$, and the entries of \mathbf{J}_{ER} are pseudo-coordinates of the complex envelopes $i_{ER1}(t), \dots, i_{ERm}(t)$. In subsection “E. Implementation” below, we explain how sensing unit output signals each proportional to a voltage or current at one of the radio ports can be processed to obtain such pseudo-coordinates, hence the entries of \mathbf{U}_{ER} and \mathbf{J}_{ER} . Once this is done, it is possible to compute \mathbf{J}_{ER}^{-1} and use (56) to obtain the wanted result: \mathbf{Z}_U at f_C .

D. SENSING UNITS AT THE ANTENNA PORTS

We now outline an example of signal processing for the configuration in which the sensing unit output signals are determined by electrical variables sensed at the n antenna ports. For simplicity, we may for instance assume that the electrical variables are the voltages and currents at the antenna ports.

For any $b \in \{1, \dots, n\}$, we can use $i_{Ab}(t)$ to denote the current flowing out of antenna port b , and $v_{Ab}(t)$ to denote the voltage across antenna port b . As explained above, $i_{Ab}(t)$ and $v_{Ab}(t)$ are bandpass signals of carrier frequency f_C . Let $i_{EAb}(t)$ and $v_{EAb}(t)$ be the complex envelopes of $i_{Ab}(t)$ and $v_{Ab}(t)$, respectively, for this carrier frequency.

For any $a \in \{1, \dots, m\}$, we can use \mathbf{u}_{EAa} to denote the column vector of the a -th pseudo-coordinates of the complex envelopes $v_{EA1}(t), \dots, v_{EAa}(t)$ in \mathcal{B} , and we can use \mathbf{j}_{EAa} to denote the column vector of the a -th pseudo-coordinates of the complex envelopes $i_{EA1}(t), \dots, i_{EAa}(t)$ in \mathcal{B} . If the bandwidth of the complex envelopes $v_{EOC_1}(t), \dots, v_{EOC_m}(t)$ is sufficiently narrow, by (46) and (51), for any $a \in \{1, \dots, m\}$, we have

$$\mathbf{j}_{EAa} \simeq \mathbf{K}(\mathbf{Z}_U + \mathbf{Z}_L)^{-1} \mathbf{E}_a, \quad (57)$$

where \mathbf{E}_a has the same meaning as above and where \mathbf{K} is a dimensionless complex matrix of size n by m , which depends on \mathbf{Z}_{Sant} , and

$$\mathbf{u}_{EAa} \simeq \mathbf{Z}_{Sant} \mathbf{j}_{EAa}. \quad (58)$$

In (57) and (58), \mathbf{K} , \mathbf{Z}_U and \mathbf{Z}_L are considered at f_C .

Let \mathbf{U}_{EA} be the complex matrix of size n by m whose column vectors are $\mathbf{u}_{EA1}, \dots, \mathbf{u}_{EAa}$, and \mathbf{J}_{EA} be the complex matrix of size n by m whose column vectors are $\mathbf{j}_{EA1}, \dots, \mathbf{j}_{EAa}$. \mathbf{U}_{EA} is dimensionless, and \mathbf{J}_{EA} has the dimensions of admittance. By (57) we have

$$\mathbf{J}_{EA} \simeq \mathbf{K}(\mathbf{Z}_U + \mathbf{Z}_L)^{-1}. \quad (59)$$

Since $\mathbf{Z}_U + \mathbf{Z}_L$ is invertible, as explained above, \mathbf{J}_{EA} is correctly determined by (59). By (58), we have

$$\mathbf{U}_{EA} \simeq \mathbf{Z}_{Sant} \mathbf{J}_{EA}. \quad (60)$$

If $m = n$, we may assume that $\mathbf{K}(\mathbf{Z}_U + \mathbf{Z}_L)^{-1}$ is invertible. In this case, it follows from (60) that

$$\mathbf{Z}_{Sant} \simeq \mathbf{U}_{EA} \mathbf{J}_{EA}^{-1}. \quad (61)$$

The entries of \mathbf{U}_{EA} are pseudo-coordinates of the complex envelopes $v_{EA1}(t), \dots, v_{EA n}(t)$, and the entries of \mathbf{J}_{EA} are pseudo-coordinates of the complex envelopes $i_{EA1}(t), \dots, i_{EA n}(t)$. In subsection ‘‘E. Implementation’’ below, we explain how sensing unit output signals each proportional to a voltage or current at one of the antenna ports can be processed to obtain such pseudo-coordinates, hence the entries of \mathbf{U}_{EA} and \mathbf{J}_{EA} . Once this is done, if $m = n$, it is possible to compute \mathbf{J}_{EA}^{-1} and use (61) to obtain the wanted result: \mathbf{Z}_{Sant} at f_C .

E. IMPLEMENTATION

To obtain \mathbf{Z}_U in subsection ‘‘C. Sensing units at the radio ports’’, we have used (56) which involves a matrix inversion. Likewise, to obtain \mathbf{Z}_{Sant} in subsection ‘‘D. Sensing units at the antenna ports’’, we have used (61) which also involves a matrix inversion. Thus, continuous-time control is not possible, and we consider a discrete-time control scheme in which we use a number $\mu \geq m$ of samples of each relevant variable to determine \mathbf{Z}_U or \mathbf{Z}_{Sant} .

For any $a \in \{1, \dots, m\}$, we may for instance assume that the μ samples $\check{v}_{EOC a}[1], \dots, \check{v}_{EOC a}[\mu]$ of $v_{EOC a}(t)$ are known as digital signals. The TSPU uses these samples to generate the excitation $v_{OC a}(t)$. The TSPU could for instance subject $\check{v}_{EOC a}[1], \dots, \check{v}_{EOC a}[\mu]$ to a digital to analog conversion producing in-phase and quadrature analog signals used for in-phase/quadrature (I/Q) modulation, either at the frequency f_C to directly obtain the excitation $v_{OC a}(t)$, or at an intermediate frequency which is up-converted to obtain the excitation $v_{OC a}(t)$. Alternatively, the TSPU could for instance subject $\check{v}_{EOC a}[1], \dots, \check{v}_{EOC a}[\mu]$ to a bandpass digital to analog conversion followed by an up-conversion, to obtain the excitation $v_{OC a}(t)$.

For any $a \in \{1, \dots, m\}$, let $\check{\mathbf{V}}_{EOC a}$ be the column vector of size μ whose entries are $\check{v}_{EOC a}[1], \dots, \check{v}_{EOC a}[\mu]$. Since, as explained above in the subsection ‘‘A. Purpose and assumptions’’, we want $v_{EOC 1}(t), \dots, v_{EOC m}(t)$ to be linearly independent, we require that $\check{\mathbf{V}}_{EOC 1}, \dots, \check{\mathbf{V}}_{EOC m}$ are linearly independent. This is possible because $\mu \geq m$.

Let $x(t)$ be any voltage or current sensed by a SU. We can assume that this SU delivers a sensing unit output signal proportional to $x(t)$. Several techniques may be used to get the samples of $x_E(t)$, denoted by $\check{x}_E[1], \dots, \check{x}_E[\mu]$. The TSPU could for instance subject $x(t)$ to an I/Q demodulation at the frequency f_C (homodyne I/Q demodulation), or to a down-conversion followed by an I/Q demodulation at an intermediate frequency (heterodyne I/Q demodulation), to obtain two analog signals: the real part of $x_E(t)$ and the imaginary part of $x_E(t)$. These analog signals may then be converted into digital signals representing the samples $\check{x}_E[1], \dots, \check{x}_E[\mu]$ of $x_E(t)$. Alternatively, the TSPU could for instance perform a down-conversion of $x(t)$, followed by a conversion into digital signals using bandpass sampling

and digital quadrature demodulation, to obtain digital signals representing the samples $\check{x}_E[1], \dots, \check{x}_E[\mu]$ of $x_E(t)$.

Let $\check{\mathbf{X}}_E$ be the column vector of size μ whose entries are $\check{x}_E[1], \dots, \check{x}_E[\mu]$. By (51), for a well-designed signal processing, we have

$$\check{\mathbf{X}}_E \simeq \sum_{a=1}^m \lambda_a(f_C) \check{\mathbf{V}}_{EOC a}. \quad (62)$$

in which we want to determine the pseudo-coordinates $\lambda_1(f_C), \dots, \lambda_m(f_C)$. There are five reasons for the \simeq symbol in (62): the \simeq symbol in (51); inaccuracies in the process used to generate the excitations $v_{OC 1}(t), \dots, v_{OC m}(t)$; inaccuracies in the process used to obtain the samples $\check{x}_E[1], \dots, \check{x}_E[\mu]$; noise in these processes; and signals or noise received by the antennas while $x(t)$ is sensed.

Let $\Lambda(f_C)$ be the column vector whose entries are $\lambda_1(f_C), \dots, \lambda_m(f_C)$, and let $\check{\mathbf{V}}_{EOC}$ be the matrix of size μ by m whose column vectors are $\check{\mathbf{V}}_{EOC 1}, \dots, \check{\mathbf{V}}_{EOC m}$. By (62), we have

$$\check{\mathbf{V}}_{EOC} \Lambda(f_C) \simeq \check{\mathbf{X}}_E. \quad (63)$$

We now want to obtain some solution of (63), regarded as an equation of unknown $\Lambda(f_C)$. A least square solution of the linear system (63) is a column vector $\Lambda(f_C)$ such that $\|\Lambda(f_C)\|_2$ is minimal among all vectors $\Lambda(f_C)$ for which $\|\check{\mathbf{V}}_{EOC} \Lambda(f_C) - \check{\mathbf{X}}_E\|_2$ is minimal, where the euclidian norm of a column vector \mathbf{V} is denoted by $\|\mathbf{V}\|_2$. The unique least square solution of (63) is

$$\Lambda(f_C) = \check{\mathbf{V}}_{EOC}^+ \check{\mathbf{X}}_E, \quad (64)$$

where \mathbf{M}^+ is used to denote the Moore-Penrose generalized inverse of a matrix \mathbf{M} [97, Sec. 7.3.P7 and Sec. 7.3.P9], [100, Sec. 4.3], [101, Sec. 5.7 and 5.8]. We required above that $\check{\mathbf{V}}_{EOC 1}, \dots, \check{\mathbf{V}}_{EOC m}$ are linearly independent. It entails that $\text{rank } \check{\mathbf{V}}_{EOC} = m$, so that $\check{\mathbf{V}}_{EOC}^* \check{\mathbf{V}}_{EOC}$ is of rank m by [97, Sec. 0.4.6], where we have used \mathbf{M}^* to denote the hermitian adjoint of a matrix \mathbf{M} . Since $\check{\mathbf{V}}_{EOC}^* \check{\mathbf{V}}_{EOC}$ is of size m by m , it is invertible so that all singular values of $\check{\mathbf{V}}_{EOC}$ are positive and

$$\check{\mathbf{V}}_{EOC}^+ = (\check{\mathbf{V}}_{EOC}^* \check{\mathbf{V}}_{EOC})^{-1} \check{\mathbf{V}}_{EOC}^*, \quad (65)$$

where we have used [100, Sec. 4.3.7]. Thus, there is no need to perform a singular value decomposition to obtain $\check{\mathbf{V}}_{EOC}^+$. It follows from (65) that $\text{rank } \check{\mathbf{V}}_{EOC}^+ = m$. This ensures that the solution given by (64) can reach any arbitrary value of $\Lambda(f_C)$. In the special case $\mu = m$, $\text{rank } \check{\mathbf{V}}_{EOC} = m$ entails that $\check{\mathbf{V}}_{EOC}$ is invertible, so that $\check{\mathbf{V}}_{EOC}^+ = \check{\mathbf{V}}_{EOC}^{-1}$.

We note that $\check{\mathbf{V}}_{EOC}^+$ can be used to process the samples of the complex envelop of all voltages and currents sensed by the SUs. Moreover, if $\check{\mathbf{V}}_{EOC 1}, \dots, \check{\mathbf{V}}_{EOC m}$ are determined in advance, they can be stored in memory, and $\check{\mathbf{V}}_{EOC}^+$ can be stored in memory so that it does not need to be computed in real time. Thus, extracting $\Lambda(f_C)$ from $\check{\mathbf{X}}_E$ requires only a matrix multiplication, so that the pseudo-coordinates of the complex envelope of each voltage or current sensed by the SUs can be easily obtained.

An important point is that there is a lot of flexibility in the choice of $\check{\mathbf{V}}_{EOC1}, \dots, \check{\mathbf{V}}_{EOCm}$, so that it is possible to use a choice which is compatible with the requirements of the standards applicable to a MIMO wireless network [85]-[87].

For $a \in \{1, \dots, m\}$, we may for instance consider the column vectors $\check{\mathbf{V}}_{CXa}$, $\check{\mathbf{V}}_{DXa}$ and $\check{\mathbf{V}}_{EXa}$, of size μ and such that

$$\check{\mathbf{V}}_{EXa} = \check{\mathbf{V}}_{CXa} + \check{\mathbf{V}}_{DXa} \quad (66)$$

where $\check{\mathbf{V}}_{CXa} \neq \mathbf{0}$, and where, for any $b \in \{1, \dots, m\}$, $\check{\mathbf{V}}_{CXa}^* \check{\mathbf{V}}_{DXb} = 0$ and $(a \neq b) \Rightarrow \check{\mathbf{V}}_{CXa}^* \check{\mathbf{V}}_{CXb} = 0$.

This assumption is for instance easily satisfied in a MIMO OFDM signal, if $\check{\mathbf{V}}_{CX1}, \dots, \check{\mathbf{V}}_{CXm}$ correspond to orthogonal reference signals existing on one or more subcarriers, and $\check{\mathbf{V}}_{DX1}, \dots, \check{\mathbf{V}}_{DXm}$ correspond to any signals existing on the other subcarriers.

For any complex numbers μ_1, \dots, μ_m such that

$$\sum_{a=1}^m \mu_a \check{\mathbf{V}}_{EXa} = \mathbf{0}, \quad (67)$$

we have, for any $b \in \{1, \dots, m\}$,

$$\check{\mathbf{V}}_{CXb}^* \sum_{a=1}^m \mu_a \check{\mathbf{V}}_{EXa} = \mu_b \check{\mathbf{V}}_{CXb}^* \check{\mathbf{V}}_{CXb} = 0. \quad (68)$$

Since $\check{\mathbf{V}}_{CXb} \neq \mathbf{0}$, we have $\check{\mathbf{V}}_{CXb}^* \check{\mathbf{V}}_{CXb} \neq 0$. It follows that $\mu_b = 0$.

Thus, $\check{\mathbf{V}}_{EX1}, \dots, \check{\mathbf{V}}_{EXm}$ are linearly independent. It follows that a possible choice of $\check{\mathbf{V}}_{EOC1}, \dots, \check{\mathbf{V}}_{EOCm}$ is $\check{\mathbf{V}}_{EOC1} = \check{\mathbf{V}}_{EX1}, \dots, \check{\mathbf{V}}_{EOCm} = \check{\mathbf{V}}_{EXm}$.

APPENDIX D

A. PURPOSE OF THIS APPENDIX AND NOTATIONS

In this Appendix D, we want to further explain and investigate different types of MAP AT control scheme which seek to obtain that \mathbf{Z}_U at f_C is very close, or as close as possible, to a wanted impedance matrix \mathbf{Z}_W .

We need to clarify the meaning of ‘‘very close, or as close as possible, to a wanted impedance matrix \mathbf{Z}_W ’’. Let us choose a matrix function, denoted by h , the matrix function being a function from a set of square complex matrices into the same set of square complex matrices, the matrix function being continuous and smooth where it is defined, and such that $h(\mathbf{Z}_W)$ is a null matrix. For instance, the function may be defined by

$$h(\mathbf{Z}) = \mathbf{Z} - \mathbf{Z}_W, \quad (69)$$

or by

$$h(\mathbf{Z}) = \mathbf{Z}^{-1} - \mathbf{Z}_W^{-1}, \quad (70)$$

or by

$$h(\mathbf{Z}) = (\mathbf{Z} - \mathbf{Z}_W)(\mathbf{Z} + \mathbf{Z}_W)^{-1}. \quad (71)$$

We say that \mathbf{Z} is (very) close to \mathbf{Z}_W if and only if a norm of $h(\mathbf{Z})$ is (very) close to zero; we say that \mathbf{Z} is as close as possible to \mathbf{Z}_W if and only if a norm of $h(\mathbf{Z})$ is as close as possible to zero; etc.

We assume a digital control system in which the nominal reactances (or equivalent variables) of the AIDs are, at a

given point in time, determined by the CU as a function of a tuning unit adjustment instruction delivered by the TSPU. An exact numerical model of the AT and of the CU may be put in the form of a mapping denoted by g_{EU} and defined by

$$g_{EU}(f, \mathbf{Z}_{Sant}, t_C, \mathbf{a}_T) = \mathbf{Z}_U, \quad (72)$$

where f is the frequency, where t_C is the applicable tuning unit adjustment instruction, and where \mathbf{a}_T is a real vector of temperatures, which is sufficient to characterize the effects of temperature on \mathbf{Z}_U .

At the frequency f and for the temperatures specified in \mathbf{a}_T , the user port impedance range of the AT is given by

$$D_{UR}(\mathbf{Z}_{Sant}) = \{g_{EU}(f, \mathbf{Z}_{Sant}, t_C, \mathbf{a}_T) | t_C \in T_C\}, \quad (73)$$

where T_C is the set of the possible tuning unit adjustment instructions [10].

B. NON-MODEL-BASED DIGITAL MAP AT CLOSED-LOOP CONTROL SCHEMES

In a non-model-based digital closed-loop control scheme (that is, a type 1 subtype b or type 2 subtype b scheme), a full automatic adjustment of the AT requires several iterations, each iteration comprising the following steps: applying excitations to the radio ports; sensing electrical variables at the radio ports; delivering a tuning unit adjustment instruction; and delivering TCSs. After a sufficient number of iterations, a final tuning unit adjustment instruction t_{CF} is reached. If the control scheme is well-designed, the measured value of \mathbf{Z}_U at f_C while t_{CF} is applicable, denoted by \mathbf{Z}_{UM} , satisfies

$$\mathbf{Z}_{UM} \simeq \mathbf{Z}_W - d_{QCL1}(f_C, \mathbf{Z}_{Sant}, t_C, \mathbf{a}_T), \quad (74)$$

where the mapping d_{QCL1} represents a quantization error which is known to the control system, but which cannot be avoided because there is no t_C in T_C such that \mathbf{Z}_{UM} is closer to \mathbf{Z}_W . Thus, the error of the control system is given by

$$\mathbf{Z}_U - \mathbf{Z}_W \simeq \mathbf{Z}_U - \mathbf{Z}_{UM} - d_{QCL1}(f_C, \mathbf{Z}_{Sant}, t_C, \mathbf{a}_T), \quad (75)$$

where $\mathbf{Z}_U - \mathbf{Z}_{UM}$ is the measurement error.

C. ADDITIONAL ASSUMPTIONS FOR MODEL-BASED MAP AT CONTROL SCHEMES

In a model-based digital control scheme (that is, a type 1 subtype c or type 3 scheme), we assume that the TSPU, instead of knowing the exact numerical model of the AT and of the CU, corresponding to g_{EU} , knows an approximate numerical model of the AT and of the CU, which corresponds to a mapping g_{AU} such that

$$g_{AU}(f, \mathbf{Z}_{Sant}, t_C, \mathbf{a}_T) + d_{AU}(f, \mathbf{Z}_{Sant}, t_C, \mathbf{a}_T) = \mathbf{Z}_U, \quad (76)$$

where the mapping d_{AU} represents the error of the approximate numerical model, and is not known to the control system.

D. TYPE 3 MAP AT CONTROL SCHEME

A type 3 control scheme uses a measurement \mathbf{Z}_{SantM} of \mathbf{Z}_{Sant} at f_C , and possibly a measurement \mathbf{a}_{TM} of \mathbf{a}_T . Here, a suitable algorithm is used to find a tuning unit adjustment instruction, denoted by t_{CS} , such that $g_{AU}(f_C, \mathbf{Z}_{SantM}, t_{CS}, \mathbf{a}_{TM})$ is very close, or as close as possible, to the wanted impedance matrix \mathbf{Z}_W . We write

$$g_{AU}(f_C, \mathbf{Z}_{SantM}, t_{CS}, \mathbf{a}_{TM}) + d_{QOL}(f_C, \mathbf{Z}_{SantM}, t_{CS}, \mathbf{a}_{TM}) = \mathbf{Z}_W, \quad (77)$$

where the mapping d_{QOL} represents a quantization error which is known to the control system, but which cannot be avoided because there is no t_C in T_C such that $g_{AU}(f_C, \mathbf{Z}_{SantM}, t_C, \mathbf{a}_{TM})$ is closer to \mathbf{Z}_W . The resulting \mathbf{Z}_U at f_C is given by

$$g_{AU}(f_C, \mathbf{Z}_{Sant}, t_{CS}, \mathbf{a}_T) + d_{AU}(f_C, \mathbf{Z}_{Sant}, t_{CS}, \mathbf{a}_T) = \mathbf{Z}_U. \quad (78)$$

Thus, the error of the control system is given by

$$\begin{aligned} \mathbf{Z}_U - \mathbf{Z}_W &= g_{AU}(f_C, \mathbf{Z}_{Sant}, t_{CS}, \mathbf{a}_T) \\ &- g_{AU}(f_C, \mathbf{Z}_{SantM}, t_{CS}, \mathbf{a}_{TM}) \\ &+ d_{AU}(f_C, \mathbf{Z}_{Sant}, t_{CS}, \mathbf{a}_T) \\ &- d_{QOL}(f_C, \mathbf{Z}_{SantM}, t_{CS}, \mathbf{a}_{TM}), \quad (79) \end{aligned}$$

in which the first 2 terms of the right-hand side vanish for exact measurements.

E. TYPE 1 SUBTYPE C MAP AT CONTROL SCHEME

In a type 1 subtype c control scheme, an adjustment sequence comprises the following steps: an initial tuning unit adjustment instruction t_{CI} is delivered by the TSPU; a measurement \mathbf{Z}_{UIM} of \mathbf{Z}_{UI} is obtained, where \mathbf{Z}_{UI} is the value of \mathbf{Z}_U at f_C while t_{CI} is applicable; and a subsequent tuning unit adjustment instruction t_{CS} is computed as explained below, and delivered by the TSPU [87]. While t_{CI} is applicable, we have

$$g_{AU}(f_C, \mathbf{Z}_{Sant}, t_{CI}, \mathbf{a}_T) + d_{AU}(f_C, \mathbf{Z}_{Sant}, t_{CI}, \mathbf{a}_T) = \mathbf{Z}_{UI}. \quad (80)$$

Let \mathbf{a}_{TM} be an estimate of \mathbf{a}_T , possibly based on a measurement. The TSPU solves the equation

$$g_{AU}(f_C, \mathbf{Z}_{SantE}, t_{CI}, \mathbf{a}_{TM}) = \mathbf{Z}_{UIM} \quad (81)$$

with respect to the unknown \mathbf{Z}_{SantE} , to obtain an estimated value \mathbf{Z}_{SantE} of \mathbf{Z}_{Sant} . Thus, we have

$$\begin{aligned} \mathbf{Z}_{UI} - \mathbf{Z}_{UIM} &= g_{AU}(f_C, \mathbf{Z}_{Sant}, t_{CI}, \mathbf{a}_T) \\ &- g_{AU}(f_C, \mathbf{Z}_{SantE}, t_{CI}, \mathbf{a}_{TM}) \\ &+ d_{AU}(f_C, \mathbf{Z}_{Sant}, t_{CI}, \mathbf{a}_T). \quad (82) \end{aligned}$$

\mathbf{Z}_{SantE} and \mathbf{a}_{TM} are then used by a suitable algorithm to determine t_{CS} such that $g_{AU}(f_C, \mathbf{Z}_{SantE}, t_{CS}, \mathbf{a}_{TM})$ is very close, or as close as possible, to the wanted impedance

matrix \mathbf{Z}_W . We note that this step is similar to the one leading to (77). We may write

$$g_{AU}(f_C, \mathbf{Z}_{SantE}, t_{CS}, \mathbf{a}_{TM}) + d_{QCL2}(f_C, \mathbf{Z}_{SantE}, t_{CS}, \mathbf{a}_{TM}) = \mathbf{Z}_W, \quad (83)$$

where the mapping d_{QCL2} represents a quantization error which is known to the control system, but which cannot be avoided because there is no t_C in T_C such that $g_{AU}(f_C, \mathbf{Z}_{SantE}, t_C, \mathbf{a}_{TM})$ is closer to \mathbf{Z}_W . The resulting \mathbf{Z}_U at f_C while t_{CS} is applicable is given by

$$g_{AU}(f_C, \mathbf{Z}_{Sant}, t_{CS}, \mathbf{a}_T) + d_{AU}(f_C, \mathbf{Z}_{Sant}, t_{CS}, \mathbf{a}_T) = \mathbf{Z}_U. \quad (84)$$

Thus, the error of the control system while t_{CS} is applicable is given by

$$\begin{aligned} \mathbf{Z}_U - \mathbf{Z}_W &= g_{AU}(f_C, \mathbf{Z}_{Sant}, t_{CS}, \mathbf{a}_T) \\ &- g_{AU}(f_C, \mathbf{Z}_{SantE}, t_{CS}, \mathbf{a}_{TM}) \\ &+ d_{AU}(f_C, \mathbf{Z}_{Sant}, t_{CS}, \mathbf{a}_T) \\ &- d_{QCL2}(f_C, \mathbf{Z}_{SantE}, t_{CS}, \mathbf{a}_{TM}), \quad (85) \end{aligned}$$

in which the first 3 terms of the right-hand side vanish for exact measurements and an exact numerical model. Let us use Λ_{AU} to denote the mapping such that

$$\begin{aligned} \Lambda_{AU}(f_C, \mathbf{Z}_{Sant}, \mathbf{Z}_{SantE}, t_{CS}, t_{CI}, \mathbf{a}_T, \mathbf{a}_{TM}) &= \\ &= g_{AU}(f_C, \mathbf{Z}_{Sant}, t_{CS}, \mathbf{a}_T) - g_{AU}(f_C, \mathbf{Z}_{SantE}, t_{CS}, \mathbf{a}_{TM}) \\ &+ d_{AU}(f_C, \mathbf{Z}_{Sant}, t_{CS}, \mathbf{a}_T) \\ &- [g_{AU}(f_C, \mathbf{Z}_{Sant}, t_{CI}, \mathbf{a}_T) - g_{AU}(f_C, \mathbf{Z}_{SantE}, t_{CI}, \mathbf{a}_{TM}) \\ &+ d_{AU}(f_C, \mathbf{Z}_{Sant}, t_{CI}, \mathbf{a}_T)]. \quad (86) \end{aligned}$$

For any values of f_C , \mathbf{Z}_{Sant} , \mathbf{Z}_{SantE} , t_{CI} , \mathbf{a}_T and \mathbf{a}_{TM} , we have

$$\Lambda_{AU}(f_C, \mathbf{Z}_{Sant}, \mathbf{Z}_{SantE}, t_{CI}, t_{CI}, \mathbf{a}_T, \mathbf{a}_{TM}) = 0. \quad (87)$$

It follows from (82) and (86) that

$$\begin{aligned} \mathbf{Z}_{UI} - \mathbf{Z}_{UIM} &+ \Lambda_{AU}(f_C, \mathbf{Z}_{Sant}, \mathbf{Z}_{SantE}, t_{CS}, t_{CI}, \mathbf{a}_T, \mathbf{a}_{TM}) = \\ &= g_{AU}(f_C, \mathbf{Z}_{Sant}, t_{CS}, \mathbf{a}_T) - g_{AU}(f_C, \mathbf{Z}_{SantE}, t_{CS}, \mathbf{a}_{TM}) \\ &+ d_{AU}(f_C, \mathbf{Z}_{Sant}, t_{CS}, \mathbf{a}_T). \quad (88) \end{aligned}$$

Substituting (88) in (85), we can write that the error of the control system while t_{CS} is applicable is given by

$$\begin{aligned} \mathbf{Z}_U - \mathbf{Z}_W &= \mathbf{Z}_{UI} - \mathbf{Z}_{UIM} \\ &+ \Lambda_{AU}(f_C, \mathbf{Z}_{Sant}, \mathbf{Z}_{SantE}, t_{CS}, t_{CI}, \mathbf{a}_T, \mathbf{a}_{TM}) \\ &- d_{QCL2}(f_C, \mathbf{Z}_{SantE}, t_{CS}, \mathbf{a}_{TM}). \quad (89) \end{aligned}$$

By (81), \mathbf{Z}_{SantE} may be regarded as a function of f_C , t_{CI} , \mathbf{a}_{TM} and \mathbf{Z}_{UIM} . Thus, by (83), t_{CS} may be regarded as a function of f_C , t_{CI} , \mathbf{a}_{TM} , \mathbf{Z}_{UIM} and \mathbf{Z}_W . Thus, by (86), $\Lambda_{AU}(f_C, \mathbf{Z}_{Sant}, \mathbf{Z}_{SantE}, t_{CS}, t_{CI}, \mathbf{a}_T, \mathbf{a}_{TM})$ may be

regarded as a function of $f_C, \mathbf{Z}_{Sant}, t_{CI}, \mathbf{a}_T, \mathbf{a}_{TM}, \mathbf{Z}_{UIM}$ and \mathbf{Z}_W . Thus, we can define the mapping E_{AU} such that

$$E_{AU}(f_C, \mathbf{Z}_{Sant}, t_{CI}, \mathbf{a}_T, \mathbf{a}_{TM}, \mathbf{Z}_{UIM}, \mathbf{Z}_W) = \Lambda_{AU}(f_C, \mathbf{Z}_{Sant}, \mathbf{Z}_{SantE}, t_{CS}, t_{CI}, \mathbf{a}_T, \mathbf{a}_{TM}). \quad (90)$$

If $\mathbf{Z}_{UIM} = \mathbf{Z}_W$, the control system believes that it has reached \mathbf{Z}_W , so that $t_{CS} = t_{CI}$. Thus, using (87) and (90), we obtain that for any values of $f_C, \mathbf{Z}_{Sant}, t_{CI}, \mathbf{a}_T, \mathbf{a}_{TM}$ and \mathbf{Z}_W , we have

$$E_{AU}(f_C, \mathbf{Z}_{Sant}, t_{CI}, \mathbf{a}_T, \mathbf{a}_{TM}, \mathbf{Z}_W, \mathbf{Z}_W) = 0. \quad (91)$$

With respect to the variable \mathbf{Z}_{UIM} of (90), the mapping E_{AU} is probably neither smooth nor continuous, because of the quantization error and possibly other reasons. However, let us assume that the control system and its numerical model are such that, with respect to the variable \mathbf{Z}_{UIM} , the mapping E_{AU} may be approximately considered as continuous. Thus, by (91), if \mathbf{Z}_{UIM} is sufficiently close to \mathbf{Z}_W , then $E_{AU}(f_C, \mathbf{Z}_{Sant}, t_{CI}, \mathbf{a}_T, \mathbf{a}_{TM}, \mathbf{Z}_{UIM}, \mathbf{Z}_W)$ is close to 0 and $\Lambda_{AU}(f_C, \mathbf{Z}_{Sant}, \mathbf{Z}_{SantE}, t_{CS}, t_{CI}, \mathbf{a}_T, \mathbf{a}_{TM})$ is close to 0. Thus, if \mathbf{Z}_{UIM} is sufficiently close to \mathbf{Z}_W , the error of the control system while t_{CS} is applicable satisfies

$$\mathbf{Z}_U - \mathbf{Z}_W \simeq \mathbf{Z}_{UI} - \mathbf{Z}_{UIM} - d_{QCL2}(f_C, \mathbf{Z}_{SantE}, t_{CS}, \mathbf{a}_{TM}). \quad (92)$$

According to (92), the error of the control system while t_{CS} is applicable is almost equal to the measurement error $\mathbf{Z}_{UI} - \mathbf{Z}_{UIM}$ less the quantization error. If we compare (92) to (89), we observe that a cancellation of errors has occurred. Also, the error given by (92) is to a large extent independent of the accuracy of the approximate numerical model, and (92) is similar to (75) established for a non-model-based closed-loop control system. This advantage is a consequence of the fact that the control system has used the approximate numerical model of the AT and of the CU twice: the first time to estimate \mathbf{Z}_{SantE} , and the second time to determine t_{CS} .

F. TYPE 1 SUBTYPE C WITH ITERATION FOR A MAP AT

Let us now assume that the adjustment sequence considered so far has used an initial tuning unit adjustment instruction t_{CI} such that \mathbf{Z}_{UIM} need not be sufficiently close to \mathbf{Z}_W to obtain that the error of the control system at the end of this first adjustment sequence satisfies (92). Thus, at the end of this first adjustment sequence, the error is given by (89). We can now introduce an iteration, in which the first adjustment sequence is quickly followed by a second adjustment sequence, such that the subsequent tuning unit adjustment instruction of the first adjustment sequence becomes the initial tuning unit adjustment instruction of a second adjustment sequence. If the first adjustment sequence is sufficiently accurate, the second adjustment sequence uses an initial tuning unit adjustment instruction such that \mathbf{Z}_{UIM} is sufficiently close to \mathbf{Z}_W to obtain that the error of the control system at the end of the second adjustment sequence satisfies (92). Thus, under this assumption, thanks to the iteration, a cancellation of errors is obtained, such that the error of the

control system at the end of the second adjustment sequence becomes to a large extent independent of the accuracy of the approximate numerical model.

REFERENCES

- [1] Y. Chen, R. Martens, R. Valkonen, and D. Manteuffel, "Evaluation of adaptive impedance tuning for reducing the form factor of handset antennas," *IEEE Trans. Antennas Propag.*, vol. 63, no. 2, pp. 703-710, Feb. 2015.
- [2] J.L. Hilbert, *Tunable RF Components and Circuits – Applications in Mobile Handsets*, Boca Raton, FL, USA: CRC Press, 2016.
- [3] W. Lam and B. Shaffer, *The RF front-end: Unsung Hero of the Premium Smartphone*, Jul. 2017 [Online]. Available: <https://technology.ihf.com>.
- [4] *HF transceiver / All-mode multi bander – TS-450S/690S – Service manual*, Tokyo, Japan: Kenwood, 1991.
- [5] *HF Antenna Tuning Unit R&S FK855U*, data sheet, Rohde & Schwarz & Co. KG, May 2006.
- [6] Y. Sun and J.K. Fidler, "High-speed automatic antenna tuning units," *Proc. IEE Ninth Int. Conf. on Antennas and Propagation*, (IEE Conf. Publ. No. 407), pp. 218-222, Apr. 1995.
- [7] E.L. Firrao, A.-J. Annema, and B. Nauta, "An automatic antenna tuning system using only RF signal amplitudes," *IEEE Trans. Circuits Syst. II, Exp. Briefs*, vol. 55, no. 9, pp. 833-837, Sep. 2008.
- [8] A. van Bezooijen, M.A. de Jongh, F. van Straten, R. Mahmoudi, and A.H.M. van Roermund, "Adaptive impedance-matching techniques for controlling L networks," *IEEE Trans. Circuits Syst. I, Reg. Papers*, vol. 57, no. 2, pp. 495-505, Feb. 2010.
- [9] E.L. Firrao, A.-J. Annema, F.E. van Vliet, and B. Nauta, "On the minimum number of states of switchable matching networks," *IEEE Trans. Circuits Syst. I, Reg. Papers*, vol. 62, no. 2, pp. 433-440, Feb. 2015.
- [10] F. Broyd e and E. Clavelier, "Some properties of multiple-antenna-port and multiple-user-port antenna tuners," *IEEE Trans. Circuits Syst. I, Reg. Papers*, vol. 62, no. 2, pp. 423-432, Feb. 2015.
- [11] G. Weale, P. McIntosh, and S. Haddow, "Closed-loop antenna tuning: why, what, where," *Proc. 2016 IEEE 5th Asia-Pacific Conference on Antennas and Propagation, APCAP 2016*, pp. 257-258, Jul. 2016.
- [12] *Dictionnaire CEI multilingue de l'electricit e – IEC multilingual dictionary of electricity, vol. 1*, Gen eve, Suisse: Bureau Central de la Commission Electrotechnique Internationale, 1983.
- [13] R. Scheer, E. Krenz, and I. Szini, "Adaptive antenna tuning systems and methods," U.S. Patent 8 204 446, filed Oct. 29, 2009.
- [14] V. True and B. Fisk, "Automatic Impedance Matching Apparatus," U.S. Patent 2 745 067, filed Jun. 28, 1951.
- [15] *The A. R. R. L. Antenna Book*, 8th edition, West Hartford, CT, USA: The American Radio Relay League, 1956.
- [16] W.B. Bruene, "Antenna Tuner Discriminator," U.S. Patent 4 493 112, filed Nov. 19, 1981.
- [17] M. Mileusni c, P. Petrovi c, and J. Todorovi c, "Design and implementation of fast antenna tuners for HF radio systems," *Proc. 1997 IEEE Int. Conf. on Information, Communications and Signal Processing (ICICS '97)*, pp. 1722-1726, Sep. 1997.
- [18] A. van Bezooijen, M. de Jongh, C. Chanlo, L. Ruijs, H. J. ten Dolle, P. Lok, F. van Straaten, J. Sneepe, R. Mahmoudi, and A.H.M. van Roermund, "RF-MEMS based adaptive antenna matching module," *Proc. 2007 IEEE Radio Frequency Integrated Circuits Symp.*, pp. 573-576, Jun. 2007.
- [19] A. van Bezooijen, M. A. de Jongh, C. Chanlo, L.C.H. Ruijs, F. van Straten, R. Mahmoudi, and A.H.M. van Roermund, "A GSM/EDGE-/WCDMA adaptive series LC matching network using RF-MEMS switches," *IEEE J. Solid-State Circuits*, vol. 43, no. 10, pp. 2259-2268, Oct. 2008.
- [20] F. Chan Wai Po, E. de Foucauld, and P. Vincent, "Method for automatic impedance matching for a radiofrequency circuit and transmission or reception system with automatic matching," U.S. patent 8 140 033, filed Sep. 10, 2008.
- [21] S.M. Ali, M.H. Bakr, and J. Warden, "Dynamic real-time calibration for antenna matching in the transmission mode", *Proc. 2010 IEEE Antenna and Propagation Society Int. Symp., APS/URSI 2010*, pp. 1-4, July 2010.
- [22] F. Chan Wai Po, E. de Foucauld, D. Morche, P. Vincent, and E. Kerherv e, "A Novel Method for Synthesizing an Automatic Matching Network and Its Control Unit," *IEEE Trans. Circuits Syst. I, Reg. Papers*, vol. 58, no. 9, pp. 2225-2236, Sep. 2011.
- [23] F. Broyd e and E. Clavelier, "Method for automatic adjustment of a tuning unit, and apparatus for radio communication using this



- method," Patent Cooperation Treaty application PCT/IB2019/056447 (WO 2020/035756), filed 29 Jul. 2019.
- [24] F. Broydé and E. Clavelier, "Method for automatically adjusting a tuning unit, and apparatus for radio communication using this method," Patent Cooperation Treaty application PCT/IB2019/056484 (WO 2020/039284), filed 30 Jul. 2019.
- [25] M. Thompson and J.K. Fidler, "Determination of the impedance matching domain of impedance matching networks," *IEEE Trans. Circuits Syst. I, Reg. Papers*, Vol. 51, No. 10, pp. 2098-2106, Oct. 2004.
- [26] Y. Sun and J.K. Fidler, "Design of Π impedance matching networks," *Proc. 1994 IEEE Int. Symp. on Circuits and Systems, ISCAS '94*, vol.5, pp. 5-8, Jun. 1994.
- [27] F. Broydé and E. Clavelier, "A tuning computation technique for a multiple-antenna-port and multiple-user-port antenna tuner," *International Journal of Antennas and Propagation*, vol. 2016, Article ID 4758486, Nov. 2016.
- [28] K.B. Ariyur and M. Krstic, *Real-Time Optimization by Extremum-Seeking Control*, Hoboken, NJ, USA: Wiley-Interscience, 2003.
- [29] C. Olalla, M.I. Arteaga, R. Leyva, and A.E. Aroudi, "Analysis and comparison of extremum seeking control techniques," *Proc. 2007 IEEE Int. Symp. on Industrial Electronics*, pp. 72-76, 4-7 Jun. 2007.
- [30] B. Calli, W. Caarls, P. Jonker, and M. Wisse, "Comparison of extremum seeking control algorithms for robotic applications," *Proc. 2012 IEEE/RSJ Int. Conf. on Intelligent Robots and Systems*, pp. 3195-3202, Oct. 2012.
- [31] C. Zhang and R. Ordóñez, *Extremum-Seeking Control and Application*, London, U.K.: Springer-Verlag, 2012.
- [32] D. Armitage, "Automatic impedance matching apparatus," U.S. Patent 4 356 458, filed Aug. 31, 1981.
- [33] D.A. Roberts and B.T. DeWitt, "Automatic antenna tuning system," U.S. Patent 5 225 847, filed Feb. 7, 1991.
- [34] Y. Sun and W.K. Lau, "Evolutionary tuning method for automatic impedance matching in communication systems," *Proc. 1998 IEEE Int. Conf. on Electronics, Circuits and Systems (ICECS 1998)*, pp. 73-77, Sep. 1998.
- [35] J. de Mingo, A. Valdovinos, A. Crespo, D. Navarro, and P. Garcia, "An RF electronically controlled impedance tuning network design and its application to an antenna input impedance matching system," *IEEE Trans. Microw. Theory Techn.*, vol. 52, no. 2, pp. 489-497, Feb. 2004.
- [36] P. Sjöblom and H. Sjöland, "An adaptive impedance tuning CMOS circuit for ISM 2.4 GHz band," *IEEE Trans. Circuits Syst. I, Reg. Papers*, vol. 52, no. 6, pp. 1115-1124, Jun. 2005.
- [37] H. Song, S.-H. Oh, J.T. Aberle, B. Bakkaloglu, and C. Chakrabarti, "Automatic antenna tuning unit for software-defined and cognitive radio," *Proc. 2007 IEEE Antennas and Propagation Society Int. Symp.*, pp. 85-88, Jun. 2007.
- [38] H. Song, B. Bakkaloglu, and J.T. Aberle, "A CMOS adaptive antenna-impedance-tuning IC operating in the 850 MHz-to-2 GHz band," *Proc. 2009 IEEE Int. Solid-State Circuits Conf.*, pp. 384-386, Feb. 2009.
- [39] L.F. Cygan, P.H. Gailus, W.J. Turney, and F.R. Yester, Jr., "Method and apparatus for enhancing an operating characteristic of a radio transmitter," U.S. Patent 5 564 086, filed Nov. 29, 1993.
- [40] G.J.L. Bouisse and J.E. Morgan, "Circuit and method for impedance matching," U.S. Patent 6 414 562, filed May 27, 1997.
- [41] F. Broydé and E. Clavelier, "Method for automatically adjusting a tunable matching circuit, and automatic tuning system using this method," U.S. Patent 9 628 135, filed Nov. 23, 2016.
- [42] Q. Gu, J.R. De Luis, A.S. Morris III, and J. Hilbert, "An analytical algorithm for pi-network impedance tuners," *IEEE Trans. Circuits Syst. I, Reg. Papers*, vol. 58, no. 12, pp. 2894-2905, Dec. 2011.
- [43] F. Broydé and E. Clavelier, "Method of automatic adjustment of a tunable matching circuit, and automatic tuning system using this method," U.S. Patent 9 935 607, filed Oct. 20, 2017.
- [44] F. Broydé and E. Clavelier, "Method of automatic adjustment of a tunable impedance matching circuit, and automatic tuning system using this method," U.S. Patent 9 966 924, filed Oct. 27, 2017.
- [45] W.E. McKinzie III, "Adaptive impedance matching apparatus, system and method," U.S. Patent 7 714 676, filed Nov. 8, 2006.
- [46] W.E. McKinzie III, "Adaptive impedance matching apparatus, system and method with improved dynamic range," U.S. Patent 7 535 312, filed Nov. 8, 2006.
- [47] W.E. McKinkie, III, "Adaptive impedance matching module," U.S. Patent 8 299 867, filed: Nov. 8, 2006.
- [48] K. Kurokawa, "Power waves and the scattering matrix", *IEEE Trans. Microwaves Theory Techn.*, vol. 13, no. 2, pp. 194-202, Mar. 1965.
- [49] J.E. Roza, "Impedance matching system," U.S. Patent 3 443 231, filed Apr. 27, 1966.
- [50] N.J. Smith, C.-C. Chen, and J.L. Volakis, "An improved topology for adaptive agile impedance tuners," *IEEE Antennas and Wireless Propagat. Letters*, vol. 12, pp. 92-95, Mar. 2013.
- [51] Q. Gu and A.S. Morris III, "A new method for matching network adaptive control," *IEEE Trans. Microwave Theory Techn.*, vol. 61, no. 1, pp. 587-595, Jan. 2013.
- [52] A. Petosa, *Frequency-Agile Antennas for Wireless Communications*, Norwood, MA, USA: Artech House, 2014.
- [53] F. Broydé and E. Clavelier, "Method for automatic adjustment of a tunable passive antenna and a tuning unit, and apparatus for radio communication using this method," U.S. Patent 9 960 491, filed Oct. 4, 2017.
- [54] F. Broydé and E. Clavelier, "Method for automatically adjusting a tunable passive antenna and a tuning unit, and apparatus for radio communication using this method," U.S. Patent 10 008 777, filed Oct. 12, 2017.
- [55] F. Broydé and E. Clavelier, "Method for automatic adjustment of a tunable passive antenna and a tuning unit, and apparatus for radio communication using this method," U.S. Patent 10 044 380, filed Nov. 2, 2017.
- [56] F. Broydé and E. Clavelier, "Method for automatically adjusting a tunable passive antenna and a tuning unit, and apparatus for radio communication using this method," U.S. Patent 9 991 911, filed Nov. 16, 2017.
- [57] F. Broydé and E. Clavelier, "Method of automatic adjustment of a tunable passive antenna and a tuning unit, and apparatus for radio communication using this method," Patent Cooperation Treaty application PCT/IB2020/055006, filed 27 May 2020.
- [58] H.A. Wheeler, "Small Antennas," in *Antenna Engineering Handbook*, R.C. Johnson, Ed., 3rd ed, New York, NY, USA: McGraw-Hill, 1993.
- [59] C.A. Desoer, "The maximum power transfer theorem for n -ports," *IEEE Trans. Circuit Theory*, vol. 20, no. 3, pp. 328-330, May 1973.
- [60] S.A. Bassam, M. Helaoui, and F.M. Ghannouchi, "Crossover Digital Predistorter for the Compensation of Crosstalk and Nonlinearity in MIMO Transmitters", *IEEE Trans. Microw. Theory Techn.*, vol. 57, no. 5, pp. 1119-1128, May 2009.
- [61] K. Hausmair, P.N. Landin, U. Gustavsson, C. Fager, and T. Eriksson, "Digital Predistortion for Multi-Antenna Transmitters Affected by Antenna Crosstalk", *IEEE Trans. Microw. Theory Techn.*, vol. 66, no. 3, pp. 1524-1535, Mar. 2018.
- [62] S.K. Dhar, A. Abdelhafiz, M. Aziz, M. Helaoui, and F.M. Ghannouchi, "A reflection-aware unified modeling and linearization approach for power amplifier under mismatch and mutual coupling," *IEEE Trans. Microw. Theory Techn.*, vol. 66, no. 9, pp. 4147-4157, Sep. 2018.
- [63] S. Stein, "On cross coupling in multiple-beam antennas," *IRE Trans. Antennas Propagat.*, vol. 10, no. 5, pp. 548-557, Sep. 1962.
- [64] J.W. Wallace and M.A. Jensen, "Termination-dependent diversity performance of coupled antennas: network theory analysis," *IEEE Trans. Antennas Propagat.*, vol. 52, no. 1, pp. 98-105, Jan. 2004.
- [65] M.L. Morris and M.A. Jensen, "Network model for MIMO systems with coupled antennas and noisy amplifiers," *IEEE Trans. Antennas Propagat.*, vol. 53, no. 1, pp. 545-552, Jan. 2005.
- [66] F. Broydé and E. Clavelier, "About the beam cosines and the radiation efficiency of a multiport antenna array," *Proc. 12th European Conference on Antenna and Propagation, EuCAP 2018*, pp. 1-5, Apr. 2018.
- [67] R. Mohammadkhani and J.S. Thompson, "Adaptive uncoupled termination for coupled arrays in MIMO systems," *IEEE Trans. Antennas Propagat.*, vol. 61, no. 8, pp. 4284-4295, Aug. 2013.
- [68] F. Broydé and E. Clavelier, "Two multiple-antenna-port and multiple-user-port antenna tuners," *Proc. 9th European Conference on Antenna and Propagation, EuCAP 2015*, pp. 1-5, Apr. 2015.
- [69] M.A. Jensen and B. Booth, "Optimal uncoupled impedance matching for coupled MIMO arrays," *Proc. First European Conf. on Antennas and Propagation, EuCAP 2006*, pp. 1-4, Nov. 2006.
- [70] Y. Fei, Y. Fan, B.K. Lau, and J.S. Thompson, "Optimal single-port matching impedance for capacity maximization in compact MIMO arrays," *IEEE Trans. Antennas Propagat.*, vol. 56, no. 11, pp. 3566-3575, Nov. 2008.
- [71] B.K. Lau and J.B. Andersen, "On closely coupled dipoles with load matching in a random field," *Proc. 2006 IEEE 17th Int. Symp. on Personal, Indoor and Mobile Radio Communications (PIMRC'06)*, pp. 1-5, Sep. 2006.
- [72] B.K. Lau, J.B. Andersen, A.F. Molisch, and G. Kritensson, "Antenna matching for capacity maximization in compact MIMO systems," *Proc. 3rd Int. Symp. on Wireless Communication Systems (ISWCS'06)*, pp. 253-257, Sep. 2006.

- [73] J.B. Andersen and B.K. Lau, "On closely coupled dipoles in a random field," *IEEE Antennas and Wireless Propagat. Letters*, vol. 5, pp. 73-75, 2006.
- [74] M.A. Jensen and B.K. Lau, "Uncoupled matching for active and passive impedances of coupled arrays in MIMO systems," *IEEE Trans. Antennas Propagat.*, vol. 58, no. 10, pp. 3336-3343, Oct. 2010.
- [75] N. Murtaza, M. Hein, and E. Zameshaeva, "Reconfigurable decoupling and matching network for a cognitive Antenna," *Proc. 41st European Microwave Conference (EuMC)*, pp. 874-877, Oct. 2011.
- [76] X. Tang, K. Mouthaan, and J.C. Coetzee, "Tunable decoupling and matching network for diversity enhancement of closely spaced antennas," *IEEE Antennas and Wireless Propagat. Letters*, vol. 11, pp. 268-271, 2012.
- [77] A. Krewski and W.L. Schroeder, "Electrically tunable mode decomposition network for 2-port MIMO antennas," *Proc. of the 2013 Loughborough Antennas and Propagation Conference (LAPC)*, pp. 553-558, Nov. 2013.
- [78] F. Broydé and E. Clavelier, "Antenna tuning apparatus for a multiport antenna array," U.S. Patent 9 621 132, filed Jun. 25, 2014.
- [79] F. Broydé and E. Clavelier, "A new multiple-antenna-port and multiple-user-port antenna tuner," *Proc. 2015 IEEE Radio & Wireless Week, RWW 2015*, pp. 41-43, Jan. 2015.
- [80] F. Broydé and E. Clavelier, "Antenna tuning apparatus for a multiport antenna array," U.S. Patent 10 187 033, filed Apr. 10, 2017.
- [81] F. Broydé and E. Clavelier, "Two reciprocal power theorems for passive linear time-invariant multiports," *IEEE Trans. Circuits Syst. I, Reg. Papers*, vol. 67, no. 1, pp. 86-97, Jan. 2020.
- [82] F. Broydé and E. Clavelier, "Corrections to 'Two reciprocal power theorems for passive linear time-invariant multiports,'" in *IEEE Trans. Circuits Syst. I, Reg. Papers*, DOI: 10.1109/TCSI.2020.2975533.
- [83] F. Broydé and E. Clavelier, "Radio communication using multiple antennas and localization variables," U.S. Patent 9 654 162, filed Oct. 15, 2015.
- [84] F. Broydé and E. Clavelier, "Method and apparatus for automatically tuning an impedance matrix, and radio transmitter using this apparatus," U.S. Patent 9 077 317, filed Nov. 24, 2014.
- [85] F. Broydé and E. Clavelier, "Method and apparatus for automatic tuning of an impedance matrix, and radio transmitter using this apparatus", U.S. Patent 10 116 057, filed Oct. 18, 2016.
- [86] F. Broydé and E. Clavelier, "Method for automatically adjusting a tuning unit, and automatic tuning system using this method", U.S. Patent 9 966 930, filed Oct. 21, 2016.
- [87] F. Broydé and E. Clavelier, "Method of automatic adjustment of a tuning unit, and apparatus for radio communication using this method", Patent Cooperation Treaty application PCT/IB2019/051501 (WO 2019/180520), filed Feb. 25, 2019.
- [88] F. Broydé and E. Clavelier, "Radio communication using tunable antennas and an antenna tuning apparatus," U.S. Patent 9 680 510, filed Oct. 20, 2015.
- [89] F. Broydé and E. Clavelier, "Method for automatically adjusting tunable passive antennas, and automatically tunable antenna array using this method", U.S. Patent 9 698 484, filed Nov. 3, 2016.
- [90] F. Broydé and E. Clavelier, "Method for automatic adjustment of tunable passive antennas and a tuning unit, and apparatus for radio communication using this method", U.S. Patent 9 929 460, filed Sep. 1, 2017.
- [91] F. Broydé and E. Clavelier, "Method for automatically adjusting tunable passive antennas and a tuning unit, and apparatus for radio communication using this method", U.S. Patent 9 912 075, filed Sep. 6, 2017.
- [92] F. Broydé and E. Clavelier, "Method of automatic adjustment of tunable passive antennas and a tuning unit, and apparatus for radio communication using this method," Patent Cooperation Treaty application PCT/IB2020/054953, filed 26 May 2020.
- [93] F. Broydé and E. Clavelier, "Radio communication using a plurality of selected antennas," U.S. Patent 10 224 901, filed Oct. 28, 2015.
- [94] F. Broydé and E. Clavelier, "Method for automatic adjustment of a tuning unit, and radio transceiver using this method," Patent Cooperation Treaty application application PCT/IB2019/052360 (WO 2019/197923) , filed 22 Mar. 2019.
- [95] F. Broydé and E. Clavelier, "Method for automatically adjusting a tuning unit, and radio transceiver using this method," Patent Cooperation Treaty application PCT/IB2019/052374 (WO 2019/197925), filed 23 Mar. 2019.
- [96] F. Broydé and E. Clavelier, "Method for automatic adjustment of tunable passive antennas, and radio transceiver using this method," Patent Cooperation Treaty application PCT/IB2019/052454 (WO 2019/197930), filed 26 Mar. 2019.
- [97] R.A. Horn and C.R. Johnson, *Matrix analysis*, Second Edition, New York, NY, USA: Cambridge University Press, 2013.
- [98] D. Tse and P. Viswanath, *Fundamentals of Wireless Communication*, New York, NY, USA: Cambridge University Press, 2005.
- [99] J.G. Proakis and M. Salehi, *Digital Communications*, Fifth Edition, New York, NY, USA: McGraw-Hill, 2008.
- [100] J.M. Ortega, *Matrix Theory*, New York, NY, USA: Plenum Press, 1987.
- [101] L. Hogben, *Handbook of Linear Algebra*, Boca Raton, FL, USA: Chapman & Hall/CRC, 2007.



FRÉDÉRIC BROYDÉ was born in France in 1960. He received the M.S. degree in physics engineering from the Ecole Nationale Supérieure d'Ingénieurs Electriciens de Grenoble (ENSIEG) and the Ph.D. in microwaves and microtechnologies from the Université des Sciences et Technologies de Lille (USTL).

He co-founded the Excem corporation in May 1988, a company providing engineering and research and development services. He is president and CTO of Excem. Most of his activity is allocated to engineering and research in electronics, radio, antennas, electromagnetic compatibility (EMC) and signal integrity. Currently, his most active research areas are automatic antenna tuners, measuring antennas and active antennas.

Dr. Broydé is author or co-author of about 100 technical papers, and inventor or co-inventor of about 80 patent families, for which 48 US patents have been granted. He is a Senior Member of the IEEE since 2001. He is a licensed radio amateur (F5OYE).



EVELYNE CLAVELIER was born in France in 1961. She received the M.S. degree in physics engineering from the Ecole Nationale Supérieure d'Ingénieurs Electriciens de Grenoble (ENSIEG).

She is co-founder of the Excem corporation, based in Maule, France. She is CEO of Excem. She is also President of Eurexcem (a subsidiary of Excem) and President of Tekcem, a company selling or licensing intellectual property rights to foster research. She is also an active engineer and researcher. Her current research area is radio communications. She has also done research work in the areas of electromagnetic compatibility (EMC) and signal integrity. She has taken part in many electronic design and software design projects of Excem.

Prior to starting Excem in 1988, she worked for Schneider Electric (in Grenoble, France), STMicroelectronics (in Grenoble, France), and Signetics (in Mountain View, USA).

Ms. Clavelier is the author or a co-author of about 80 technical papers. She is co-inventor of about 80 patent families. She is a Senior Member of the IEEE since 2002. She is a licensed radio amateur (F1PHQ).

◆◆◆